



Review

Nanotechnology Applied to Thermal Enhanced Oil Recovery Processes: A Review

Oscar E. Medina ¹, Carol Olmos ¹, Sergio H. Lopera ², Farid B. Cortés ^{1,*}
and Camilo A. Franco ^{1,*}

¹ Grupo de Investigación en Fenómenos de Superficie—Michael Polanyi, Departamento de Procesos y Energía, Facultad de Minas, Universidad Nacional de Colombia, Sede Medellín, Medellín 050034, Colombia; oemedinae@unal.edu.co (O.E.M.); carolmaritza1@gmail.com (C.O.)

² Grupo de Yacimientos de Hidrocarburos, Departamento de Procesos y Energía, Facultad de Minas, Universidad Nacional de Colombia, Medellín 050034, Colombia; shlopera@unal.edu.co

* Correspondence: fbcortes@unal.edu.co (F.B.C.); caafrancoar@unal.edu.co (C.A.F.)

Received: 2 November 2019; Accepted: 29 November 2019; Published: 9 December 2019



Abstract: The increasing demand for fossil fuels and the depleting of light crude oil in the next years generates the need to exploit heavy and unconventional crude oils. To face this challenge, the oil and gas industry has chosen the implementation of new technologies capable of improving the efficiency in the enhanced recovery oil (EOR) processes. In this context, the incorporation of nanotechnology through the development of nanoparticles and nanofluids to increase the productivity of heavy and extra-heavy crude oils has taken significant importance, mainly through thermal enhanced oil recovery (TEOR) processes. The main objective of this paper is to provide an overview of nanotechnology applied to oil recovery technologies with a focus on thermal methods, elaborating on the upgrading of the heavy and extra-heavy crude oils using nanomaterials from laboratory studies to field trial proposals. In detail, the introduction section contains general information about EOR processes, their weaknesses, and strengths, as well as an overview that promotes the application of nanotechnology. Besides, this review addresses the physicochemical properties of heavy and extra-heavy crude oils in Section 2. The interaction of nanoparticles with heavy fractions such as asphaltenes and resins, as well as the variables that can influence the adsorptive phenomenon are presented in detail in Section 3. This section also includes the effects of nanoparticles on the other relevant mechanisms in TEOR methods, such as viscosity changes, wettability alteration, and interfacial tension reduction. The catalytic effect influenced by the nanoparticles in the different thermal recovery processes is described in Sections 4, 5, 6, and 7. Finally, Sections 8 and 9 involve the description of an implementation plan of nanotechnology for the steam injection process, environmental impacts, and recent trends. Additionally, the review proposes critical stages in order to obtain a successful application of nanoparticles in thermal oil recovery processes.

Keywords: catalysts; enhanced oil recovery; EOR; nanoparticles; nanotechnology; thermal methods

1. Introduction

According to the International Energy Agency (IEA), the world's demand for fossil fuels is expected to increase by about one-third by the year 2035 [1]. Currently, light crude oil reserves are the main energy source that supplies the global energy demand due to its high quality as well as low production cost. Nevertheless, light crude oil reserves are depleting [2,3]. In this sense, exploitation of heavy oil (HO) and extra-heavy oil (EHO) has been considered an interesting strategy to supply the energy demand since these reservoirs are approximately of the same order than conventional crude oil [4]. However, low American Petroleum Institute (API) gravities (<20° API), high viscosities

(>100,000 cp at 25 °C) of the HO and EHO as well as geological difficulties, increase the costs of production, transportation, and refining in comparison with conventional hydrocarbons [5,6]. HO and EHO are characterized by having a high percentage of asphaltenes (>15% by mass) and resins (>40% by mass), as well as a relatively low proportion of low molecular weight compounds. Besides, it may also have high contents of pollutants like sulfur and nitrogen, metals like nickel, vanadium, and iron, salts, low H/C ratio and produces more than 50% by mass of residue with boiling points above 500 °C. Its high viscosity causes multiphase flow, pipes clogging, high pressure drops, and production stops [7].

Currently, due to high reserves of Canadian oil sands, Venezuelan heavy oils, and UK continental Shelf, the HO and EHO production has received great attention from the oil and gas industry. In South America, Colombia is the third largest oil producer in the region [7]. Within national production, more than 50% is framed in the production of HO and EHO. Within the Llanos Basin, in the Chichimene located at the east central Colombia, there were estimated 1.8940×10^{10} barrels of original oil in place (OOIP), including HO and EHO [8]. Besides, Capella field, located in the North part of Caguan-Putumayo basin, produces a heavy oil with average gravity of 9° API and viscosities between 2500 and 4000 cp at reservoir conditions (56 °C and 1250 psi) [9]. Within the first processes used for artificial lift wells producing EHO and HO, progressive cavity pumps (PCP) and electro submersible pumps (ESP) are used. Notwithstanding, fluid viscosity affects the power consumption of an ESP motor and directly the efficiency of the technique, increasing the energy consumption, and the PCP systems require longer stabilization time compared with ESP equipment [10]. Hence, the development of cost-efficient technologies for heavy crude oil recovery is challenging nowadays.

Improved oil recovery (IOR) and enhanced oil recovery (EOR) methods have been developed to increase the oil production and reserves [5]. IOR strategies are used to recover mobile crude oil and/or immobile crude oil in the near wellbore, while EOR methods are employed to recover mostly immobile crude oil that remains in the reservoir after application of primary and secondary methods [11]. Major EOR technologies categories are chemical, gas, and thermal methods [12]. Chemical injection of surfactant, polymer, and solvents are the mostly used EOR methods. Nevertheless, the efficiency of the chemical injection is affected mainly by adsorption and/or degradation in the porous medium, reducing the cost/benefit ratio [13–15], and in most cases these processes are not suitable for immobile heavy and extra-heavy crude oil and oil sands [16].

Gas methods use hydrocarbon gases (CH_4 , C_3H_8 , or natural gas) or nonhydrocarbon gases (N_2 or CO_2) that dissolve in crude oil and improve its recovery by decreasing oil viscosity and expanding oil volume [17–20]. The theory behind these processes is the HO and EHO viscosity reduction caused by the dissolving of the gas injected and, thus, the displacement efficiency is improved. However, the unfavorable viscosity ratio CO_2 , N_2 , CH_4 , C_3H_8 /HO-EHO leads to a combination of gas fingering and gravity override through more permeable zones, achieving to early gas breakthrough and, ultimately, less oil being recovered [20,21]. The same behavior for EOR is observed by surfactant flooding [16].

In this order, gas and chemical injection often lead to poor mobility control and severe viscous fingering mainly in heavy and extra-heavy crude oils due to the high viscosities, resulting in insufficient sweep and displacement efficiencies [22]. In addition, chemical processes are limited to the high cost of products, potential sources of formation damage, and losses of the chemicals in the reservoir [23]. Thermal methods consist in the introduction of heat into heavy crude oil reservoirs by different methods such as, but not limited to, cyclic steam stimulation (CSS) [17,24], steam flooding, and steam-assisted gravity drainage (SAGD), where horizontal wells are applied to optimize the production process [25,26] and/or in-situ combustion (ISC) [7,23,27,28], which are summarized in Table 1.

Table 1. Conventional methods of thermal enhanced oil recovery, mechanisms, and limitations.

Method	EOR Mechanism	Limitation
Cyclic steam stimulation (CSS)	Viscosity reduction	High energy cost
In-situ combustion (ISC)	Distillation and breaking of heavy crude oil fractions	Heat leakage to the undesired layers
SAGD	Oil expansion	Low effective thermal degradation
Electrical heating	Gravity drainage	Heat loss from heat generator to the reservoir

These methods allow the mobility of heavy crude oil or bitumen in reservoirs by changing some properties such as viscosity and density. Nevertheless, thermal methods involve a large inversion in heat generation, injection, and recycling facilities that increase the operational costs [6]. To decrease the cost of HO recovery, new and novel methods that involve nanotechnology have been developed [29]. The use of nanotechnology in thermal processes emerges as an alternative for extra-heavy and heavy crude oils upgrading and recovery, which may lead to low energy consumption, less environmental impacts, and a high recovery factor [29,30]. Recently, metal and metal oxide nanoparticles (NPs) have been evaluated for asphaltene sorption and subsequent catalytic decomposition. The results have shown that nanocatalysts can considerably reduce the decomposition temperature of the asphaltenes as well as the effective activation energy, confirming their catalytic activity toward decomposition of long-chain hydrocarbons towards lighter fractions with smaller molecular weight, which implies viscosity reduction and mobility improvement of the producing heavy crude oils [31,32]. The partial upgrading of heavy crude oil is related to many types of catalytic processes such as thermal cracking [33,34], aquathermolysis [24,35], hydrocracking [36], oxidation [37–42], pyrolysis [38,42–44], and steam gasification [30,45–49].

Although the thermal recovery of heavy crude oil with nanoparticles is a relatively new technology, this has been widely investigated [23,30,44,50–54]. However, to the best of our knowledge, there is no detailed information in the scientific literature on the influence of nanomaterials for the upgrading of heavy and extra-heavy crude oils in enhanced thermal recovery techniques. In this context, the main objective of this work is to show the catalytic influence of different nanomaterials under different atmospheres such as air, steam, and inert atmospheres applied in CSS, steam flooding SAGD, and/or ISC thermal processes for the upgrading of HO and EHO based on an exhaustive review. For this, the work is divided into nine important sections. The first section has a description of the physical-chemical properties of HO and EHO and the decomposition of its heavy fractions in the absence of nanoparticles. In the second section, the interactions generated between the nanoparticles and the asphaltenes and the variables that can influence the adsorptive phenomenon are presented in detail. The third, fourth, fifth, and sixth sections describe the catalytic effect that the nanoparticles generate in the processes of thermal recovery by decomposing this fraction of the crude oil under steam, air, and inert gas injection processes, as well as electromagnetic heating, respectively. Section 7, Section 8, Section 9 describe the applicability of nanofluids and nanoparticles nanotechnology under field conditions, environmental impacts, and emerging trends. It is expected that this review opens a new panorama towards the application of nanotechnology to heavy crude oil upgrading and recovery by thermal processes.

2. Physical-Chemical Properties of Heavy (HO), Extra-Heavy Crude Oil (EHO)/Bitumen

Heavy and extra-heavy crude oils have specific properties that make them problematic in production, transport, and refinery operations [6,7,55]. These crude oils have very high viscosity values, which prevents them from flowing easily through the porous media and the production and transport lines. In addition, they have low values of American Petroleum Institute (API) gravity ($EHO < 20^\circ$ and $HO < 10^\circ$), which implies higher specific gravity values compared to light oils [44,56–58]. The main cause of the problems presented by heavy crude oils and bitumen is the high content of heavy fractions such as asphaltenes and resins in their molecular structure. Crude oil components are generally

categorized as saturates, aromatic, resins, and asphaltenes (SARA) [59,60]. The saturated compounds are the nonpolar fraction of the crude oil, and it comprises linear, branched, and cyclic saturated hydrocarbons [61]. Aromatics are the nonpolar fraction that contains aromatic rings in its molecular structure [60]. On the other hand, asphaltenes are the polar component of the crude oil and together with the resins compose the heaviest fraction, leading to high production and refinery costs [62,63]. The resins differ from the asphaltenes, in that the former is soluble in *n*-paraffins (*n*-heptane, *n*-pentane among others), while the asphaltenes are insoluble in these compounds and soluble in aromatics such as toluene and benzene [64]. Additionally, asphaltenes have a high content of heteroatoms (N, O, S) and metals (Ni, Fe, V) located close to each other, which allows them to generate a dipole moment triggering the self-association of these molecules [65,66]. Several chemical structures of asphaltenes have been proposed, such as island, archipelago, continental, or rosary-type molecules [67]. The first structure is composed of one polycyclic aromatic hydrocarbon (PAH) core and seven fused rings, while the archipelago type structure is composed of more than one PAH connected by alkyl chains [68].

On the other hand, the continental architecture is composed by a big PAH of more than seven fused rings [69]. The rosary-type is composed of more than two PAH and with flexible aliphatic chains [68,69]. Recent research suggests that asphaltenes, in general, are a mixture of two main fractions, A₁ and A₂. The A₁ fraction represents about 70% of the mixture and has low solubility in toluene (90 mg·L^{−1}). The A₂ fraction has a high solubility (57 g·L^{−1}), which is very similar to the solubility of the total mixture. In response to this definition, it should be noted that the strong trend of aggregation of asphaltenes is due to the presence of the insoluble fraction (A₁), which is present in lower quantity [70]. In this sense, studying the colloidal aggregation processes of A₁ and A₂ fractions allows an understanding of the properties of the total asphaltene fraction [71]. Nuclear magnetic resonance spectroscopy (NMR) studies combined with elemental analyses suggests that there are structural differences for the A₁ and A₂ fractions, such as those shown in the M₁ and M₂ models, where the molecular structure of the M₂ was constructed from the opening of two aliphatic rings in M₁ [70]. The proposed molecular models M₁ and M₂ for the graphical description of asphaltene fractions A₁ and A₂, respectively, are shown in Figure 1.

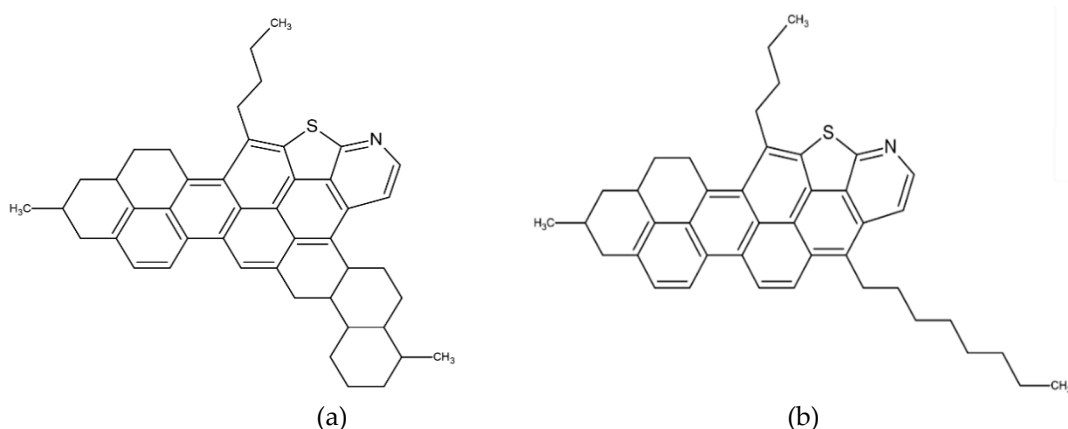


Figure 1. Molecular models (a) M₁ and (b) M₂ used to represent asphaltene fractions A₁ and A₂, respectively. Reprinted with permission [70]; Copyright 2018, ACS Publications.

From Figure 1 is observed that the A₁ fraction is formed by the bond of aromatic and aliphatic rings, which suggests a nucleus composed of polycyclic and naphthenic aromatic units (PANU), fused in a large flat nucleus. In the case of the A₂ fraction, a large number of aromatic carbons is observed, and the presence of small amounts of PANU bound by aliphatic chains is suggested [70]. In this way and from a qualitative point of view, it can be expected that a material represented by the M₂ model should have greater solubility than the M₁ model. Consistent with these ideas, it should be noted that the A₁-based aggregates form at very low concentrations and the addition of A₂ on these aggregates

prevents their growth beyond the colloidal size, i.e., keeps the A_1 molecules dispersed [70]. In this sense, Figure 2 shows a model of molecular mechanisms that simulate the nanoaggregates between four asphaltene A_1 molecules represented under the M_1 model and three A_2 represented under the M_2 model.

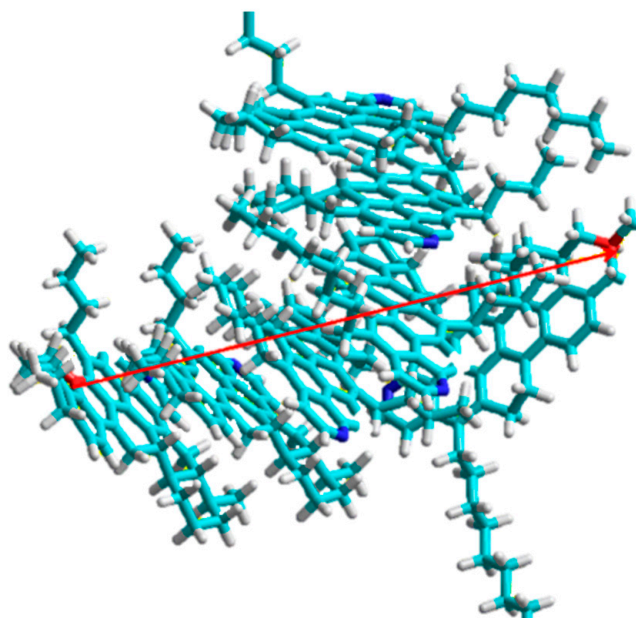


Figure 2. Graphical representation under a molecular model of an asphaltene nucleus or nanoaggregate composed of three M_2 -type molecules and four M_1 -type molecules. The length of the red line is 2.9 nm. Reprinted with permission [70]; Copyright 2018, ACS Publications.

However, the stability of asphaltenes depends to a large extent on the content of resins present in the crude oil matrix, because they can avoid asphaltene–asphaltene interactions by positioning on the surface of the asphaltene aggregate, penetrating its microporous structure and finally breaking the aggregation system [72–74]. Previous studies have reported that higher adsorption of the resins on the colloidal fractions showing a higher affinity for A_1 than for A_2 , indicating that the resin– A_1 interactions are more favorable than the A_1 – A_1 interactions [70]. At the beginning, the A_2 molecules keep the A_1 aggregates in dispersion by a steric effect. However, after the resins enter the surface of A_1 , they generate competition for their active sites together with A_2 , which generates an interfacial destabilization of the dispersion that ends at the union of the flocs of A_2 and the successive aggregation, now surrounded, by resin molecules [75].

On the other hand, the resins are classified as resin I and resin II (Figure 3). In general, resins II have a higher carbon number and hydrogen per average molecule. However, the H/C ratio is lower, which indicates its greater degree of unsaturation. Considering the aromatic carbons per molecule, a greater number is observed in resins II, which indicates that these structures have greater aromaticity [76]. If the aromatic hydrogens are compared, it is possible to affirm that due to its decrease, the resins I have a high condensation of the aromatic structure.

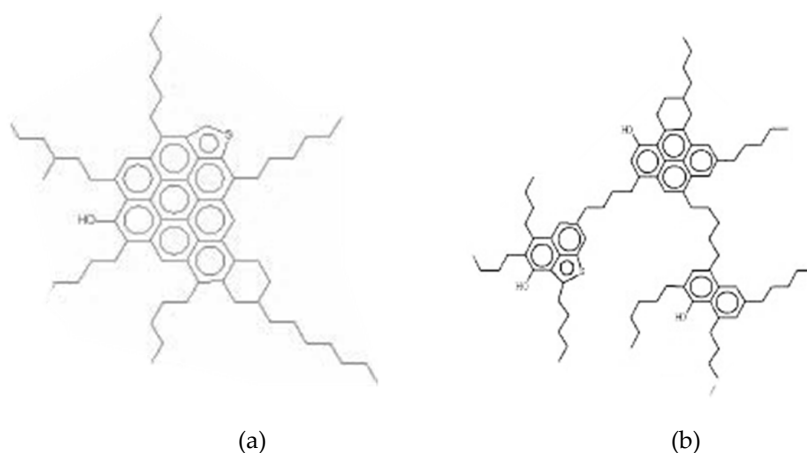


Figure 3. Molecular structure for (a) resin I and (b) resin II of Castilla crude oil. Molecular characteristics: $H/C = 1.49$ and $H/C = 1.40$ for resin I and resin II, respectively. The average molecular weight of resin I is between 500 and 900 Da and for resin II between 700 and 1300 Da. Aromaticity factor is equal to 0.57 and 0.32 for resins I and II, respectively. Reprinted with permission [76]; Copyright 2004, Ecopetrol S.A.

The length of the alkyl chains shows that the resins II have a greater number of carbons associated, indicating a greater length. Resin I, according to several studies, has a preference for precipitating with the asphaltenes of crude oil [77]. The alkyl chains and the heteroatoms present in the molecule help to generate the molecular interactions with the asphaltenes, forming in this way aggregates, where there are trapped lighter molecules that inevitably are dragged during the precipitation of these fractions [76].

However, heavy and extra-heavy crude oils commonly do not exhibit problems of asphaltene precipitation and deposition due to the high content of asphaltenes and resins lead to the formation of a viscoelastic network that reduces the flow of crude oil due to the high viscosities [78]. In this sense, enhanced oil recovery (EOR) methods have been developed to facilitate the extraction of this type of crude oil by thermal processes that allow decomposing the asphaltene molecules or interrupt the viscoelastic network to generate reductions in viscosity [79,80]. The process involves the decomposition of the asphaltene molecules by effect of elevated temperatures under different atmospheres such as air [40,45,81,82], steam [83,84], inert [44,85,86], and air/steam. Figure 4 shows a thermogravimetric analysis of the asphaltenes under different atmospheres.

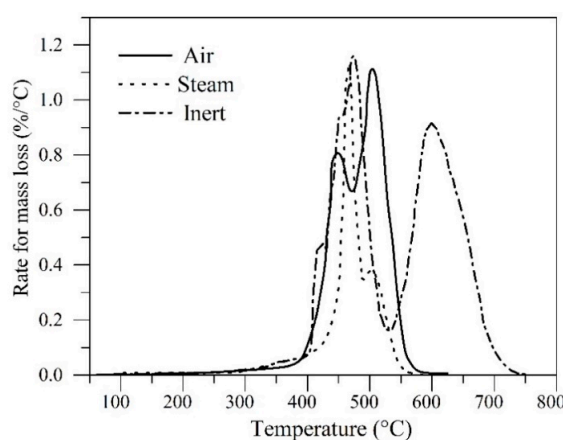


Figure 4. Comparison of rate of mass loss for $n\text{-C}_7$ asphaltenes under different atmospheres such as steam [49], inert gases [44], and air [82] performed at atmospheric pressure. Adapted with permission from Cardona et al. [49], Nassar et al. [44], and Franco et al. [82].

As can be seen, under the three atmospheres, the cracking of the asphaltenes occurs at several stages, and they start at 400, 426, and 465 °C for inert, air, and steam atmospheres, respectively [44,82,87]. Several authors explain this phenomenon due to the presence of a distribution of sizes of asphaltenes of high to low molecular weight, where the heavier fractions decompose at higher temperatures [30,45,88] and the different intensities of the different peaks is attributed to possible addition or aggregation reactions of *n*-C₇ asphaltene after its initial cracking. After the asphaltene molecules are subjected to thermal processes involving oxidation, pyrolysis, gasification reactions, and coke formation can be generated. In both pyrolysis and gasification, coke yield of 61.2% [33] and 63.3% [38] can be generated, respectively, while oxidation completely inhibits the formation of this residue. To understand this phenomenon in greater detail, Figure 5 shows a basic scheme of the reaction associated with the oxidation temperature of asphaltenes and describes the decomposition of these molecules into lighter fractions by means of two main ways: oxygen and free radicals [89]. Once the hydrocarbon molecules react with the oxygen, lighter hydrocarbon chains are formed. In the first stage, hydrocarbon branched with alcoholic and aldehyde groups are formed. Then, the reaction can take two routes. In route 1, CO can be generated resulting in R-CO• radicals and subsequently CO is released. In the route 2, the -CHO groups are further oxidized into compounds containing carboxyl groups, and carboxyl groups are broken off from the main hydrocarbon chains to generate CO₂.

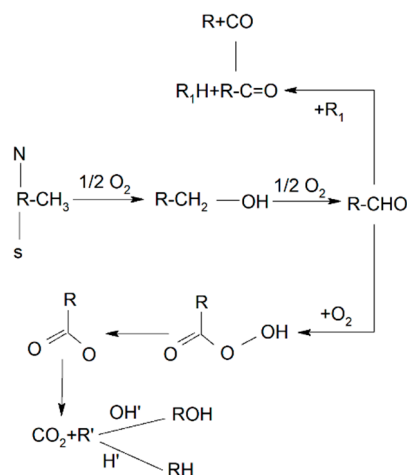


Figure 5. Basic scheme of the reaction associated with the oxidation of asphaltenes and the catalytic effect of the nanoparticles. Route 1: R-CO• radicals are generated, and CO is released, Route 2: -CHO groups are oxidized into compounds containing carboxyl groups, and CO₂ is generated.

On the other hand, the oxidation of resins has also been studied [73]. Unlike asphaltenes, the decomposition under oxidation conditions of the resin I molecules from a 6.2° API EHO of starts at much lower temperatures, around 200 °C, because the resin has a higher content of aliphatic compounds than asphaltenes molecules [73]. Additionally, the second peak of greater intensity is found at approximately 500 °C and peaks of lower intensity between 380 and 450 °C where the oxidation of the heavier molecules present in the molecular structure of the resins is generated. Additionally, the gasification of resins II and complex systems R:A (Resins: Asphaltenes) under isothermal and nonisothermal conditions, at temperatures below 240 °C. The authors found that the increase in content of resins II in the systems decreases the activation energy to carry out the decomposition of the system. Finally, considering the above, it is important to decompose these molecules in order to bring the crude oil to better viscosity conditions and API gravity to facilitate production, refinery, and transport operations [88]. However, the conventional thermal enhanced oil recovery processes do not generate an upgrading in the crude oil quality, due to the low temperatures at which it operates, since asphaltene and resins decompose mainly at temperatures above 400 °C [88].

3. Interaction between Heavy Crude Oil Fractions and Nanoparticles

It is important to study the adsorption of asphaltenes and resins over nanoparticles mainly for two reasons: (i) depending on the affinity that they have for the nanoparticle, they can be eliminated from the heavy and extra-heavy crude oils and, therefore, making the remaining fraction feasible for production and transport through reduction of viscosity and increase in API gravity values without a source of external heat in the reservoir [90–94], and (ii) the catalytic properties of the nanoparticles could facilitate catalytic decomposition reactions resulting in lighter components in the crude oil [29]. To understand the mechanism of interaction between nanoparticles and the heavy fractions of crude oil, it is important to remember that the aggregation of asphaltenes at low concentrations combined with the slow growth of these aggregates above the initial concentration is what allows reaching the solubility concentration of subfraction A₁ at approximately 90 mg·L^{−1} [70]. That is, close to this concentration a formation of nuclei formed by subfraction A₁ occurs that is surrounded by subfraction A₂ and allows it to be kept soluble [70]. It leads to the nucleation and growth of subfraction A₁ is not very soluble and it is able to be solubilized because the subfraction A₂ surrounds it, preventing a higher aggregation. When the nanoparticles contact with the heavy crude oil fractions, they can act directly in the A₁ fraction preventing their growth by the aggregation of the nuclei, because the interactions generated between NPs-A₁ subfraction are stronger than A₁-A₁ interactions by the presence of different functional groups on the surface of the nanoparticles [70,95].

Hence, several authors have studied and used a wide range of materials for the asphaltene adsorption, and especially the nanoparticles have shown a better performance as composite and/or functionalized materials. The effect of several variables in adsorption processes such as the contact time [96], heptane/toluene ratio [97], initial concentration of asphaltenes and/or nanoparticles, pressure/temperature [98,99], concentration of other fractions such as resins [100], among others, have been studied. The implementation of γ -Al₂O₃ nanoparticles [96] is one of the first studies that contemplate the use of nanoparticles for the adsorption of asphaltenes. This nanomaterial presented rapid adsorption of the heavy fraction, approaching the equilibrium in 2 h for the different concentrations of *n*-C₇ asphaltene used (100, 500, and 1000 mg·L^{−1}). In addition, the obtained adsorption isotherms were Type I, indicating a high affinity between the adsorbent and the adsorbate, with an adsorbed amount of 2.18 mg·m^{−2} for a concentration in the equilibrium C_E of 3200 mg·L^{−1} approximately. Finally, the thermodynamic studies showed that the adsorption is spontaneous and exothermic nature [96]. In addition, the modification of the surface acidity of the nanoparticle also generates an effect on the interactions with asphaltenes. The alumina nanoparticles, when modified, acquire new chemical structures on their surface as shown in Figure 6.

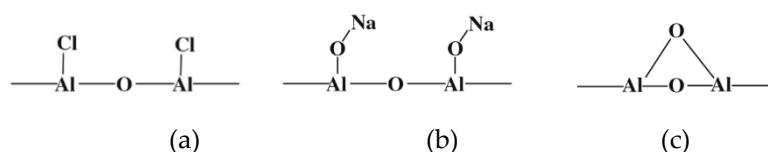


Figure 6. Chemical structure for alumina (a) acid, (b) basic, and (c) neutral. Reprinted with permission [101]; Copyright 2011, Elsevier.

The results evidenced that asphaltene adsorption followed the order: acidic > basic > neutral surfaces. This is mainly due to (i) the different counterions present in the nanoparticle surface and (ii) that the interactions for acidic alumina with polar asphaltenes can be very strong and give rise to molecular associations such as a weak chemical bond [101]. In addition, Franco et al. [40] evaluated the effect of the surface acidity in asphaltene adsorption over silica nanoparticles, and they found a higher affinity for asphaltene adsorption for acidic silica nanoparticles, followed by basic and neutral, according to the results reported by other studies [96].

Different types of nanostructured iron oxides have also been investigated, such as magnetite ($\gamma\text{-Fe}_2\text{O}_3$), hematite ($\alpha\text{-Fe}_2\text{O}_3$) [102], or iron (II, III) oxide (Fe_3O_4). The results showed that the magnetite nanoparticles (MNP) have a maximum adsorption capacity of $108.1 \text{ mg}\cdot\text{g}^{-1}$ while those of hematite (HNP) have a maximum adsorption capacity of $458 \text{ mg}\cdot\text{g}^{-1}$. Adsorption kinetics studies show that the process in the presence of HNPs reaches equilibrium faster than for MNPs, which indicates that structural differences generate an effect on the adsorption process. Finally, the nature of the adsorptive phenomenon over HNP and MNP nanoparticles is exothermic and endothermic, respectively [102].

Nickel-based or nickel-containing nanomaterials have also been used in this area. The size of NiO nanoparticles was evaluated in the adsorption of Quinolin-65 by Marei et al. [103]. The results of experimental adsorption isotherms confirmed that nanoparticles with large size (80 nm) have the highest adsorption capacity, while 5 nm size particles have the lowest. In addition, through computational modeling, a better understanding of the Q-65 interaction with NiO nanoparticles was obtained. The results indicate that, by changing the nanometric size between 5 and 80 nm, NiO nanoparticles undergo dramatic changes in surface and textural properties, which consequently affect their adsorption behavior [103]. Supports of fumed silica [82], titania, and alumina [45] for nickel and palladium nanoparticles dosed with a mass fraction of 1% of each one, showed adsorbed amounts of 0.52 , 3.11 , and $1.67 \text{ mg}\cdot\text{m}^{-2}$, respectively, while for the supports without metals on their surface, the maximum amounts adsorbed are 0.35 , 2.78 , and $1.3 \text{ mg}\cdot\text{m}^{-2}$, respectively. The improvement in the adsorptive capacity is due to the dispersion and stabilization of the asphaltenes on the surface of the nanoparticles, in addition to having a heterogeneous adsorbent with multiple selectivities. Besides, Janus-type nanoparticles impregnated with a fraction mass of 15% have been employed to evaluate the adsorption capacity and affinity with asphaltene molecules. Figure 7a shows a TEM image of the synthesized Janus nanoparticles with a partial roughness that can be seen on the half surface, which correspond to the nickel oxide on the NPs surface. Figure 7c shows the adsorption isotherms from these nanoparticles. It is possible to see an increase in the capacity of adsorption of the Janus nanoparticle compared with those of silica which can be attributed to the intermolecular forces present between the more polar components of the asphaltenes and the Ni-O bonds and silanol groups on the surface of the particles [104].

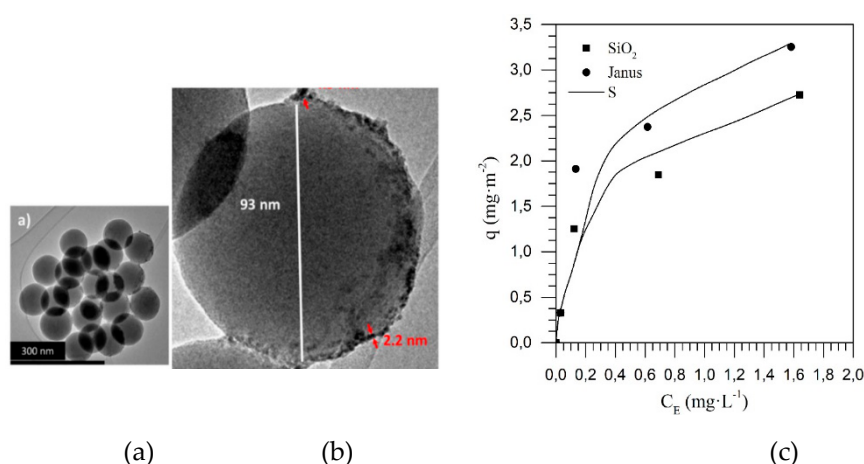


Figure 7. TEM image of Janus nanoparticles synthesized (a) general view, (b) side view, and (c) adsorption isotherms of asphaltenes on silica nanoparticles and Janus type at 25 °C. C_E (mg·L⁻¹) is the concentration at equilibrium of the asphaltene and q (mg·m⁻²) represents the adsorbed amount of asphaltenes over nanoparticles. Adapted with permission from Giraldo et al. [105], and Rebeka Diez et al. [104].

Other organic-based nanoparticles have also been studied, such as carbon nanospheres (CNS), whose adsorptive capacity is affected by the resorcinol/catalyst ratio (R/C), a high value of R/C implies greater asphaltene adsorption. Additionally, the impregnation of these nanospheres with

$(\text{NH}_4)_{10}\text{H}_2(\text{W}_2\text{O}_7)_6$ increases the adsorption capacity of nanomaterial and its affinity for asphaltenes. Comparative studies to evaluate nanoparticles of different natures have been reported in the literature [41,83,106]. Several types of silica nanoparticles (amorphous, fumaric, crystalline, and commercial) were compared with alumina nanoparticles, among which, SiO_2 showed higher asphaltene adsorption, and with the dosage of a mass fraction of 5% and 15% of nickel, increase their adsorptive capacity [106]. As for metal oxides nanoparticles, the adsorption increases in the order $\text{TiO}_2 < \text{NiO} < \text{MgO} < \text{Fe}_3\text{O}_4 < \text{Co}_3\text{O}_4 < \text{CaO}$ [107]. Finally, among the variables that can affect the adsorption of asphaltenes on nanoparticles, is the effect of resins I. In addition, resin adsorption and the effect of resins in asphaltene adsorption over silica [107], hematite [107], silica functionalized with 1% in a fraction mass of NiO and PdO [73] were evaluated. Franco et al. [73] showed that the resin adsorption, as an individual component, depends on its affinity for the nanoparticle and nature thereof. Furthermore, the adsorption of asphaltenes in the presence of resins is not affected by changes in their colloidal state if not by the affinity between the resin and the nanoparticle.

The property that allows understanding the adsorption phenomenon between asphaltenes and nanoparticles is Polanyi's potential. Polanyi's theory of physical adsorption is defined as an adsorption energy thermodynamically equal to the negative value of the free energy of change of the asphaltenes from the bulk phase to the adsorbent state [108]. Polanyi's potential is independent of temperature for a given adsorption volume, described by Equation (1).

$$\left(\frac{\partial A}{\partial T}\right)_{N_{ads}} = 0, \quad (1)$$

where, T is the temperature (K), A represents the adsorption potential ($\text{J}\cdot\text{mol}^{-1}$), and N_{ads} is the adsorbed amount in $\text{mg}\cdot\text{g}^{-1}$. This parameter allows the construction of a representative curve for each adsorbate-adsorbent couple of adsorbed amount as a function of the Polanyi's potential values. Figure 8 shows a graphical representation of the asphaltene disaggregation phenomenon when it takes contact with the nanoparticles.

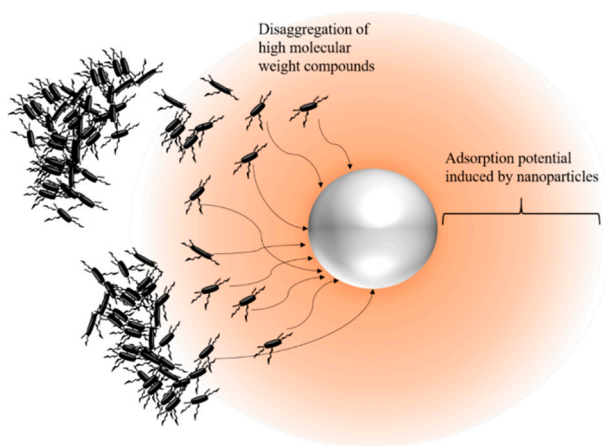


Figure 8. Asphaltene disaggregation through adsorption mechanism on nanoparticles.

Regarding the asphaltene molecular structure, commonly they are composed of aliphatic and aromatic structures. The aromatic part is a polynuclear aromatic moiety, while the aliphatic region contains alkyl chains with variable length, being the first region surrounded by the second. The attraction of the asphaltene molecules is related to the π - π and H-bond interactions between the aromatic structures. By contrast, aliphatic chains induce steric repulsion between the aromatic sheets. It means that the presence of polar and nonpolar groups promote their amphiphilic nature and self-association.

Asphaltenes tend to adsorb over solid surfaces as individual molecules or like colloidal aggregates of different sizes due to their carboxylic and phenolic acid groups. The favorable adsorption of

asphaltenes over nanoparticles occurs because of the forces formed by functional groups of the nanoparticles employed and the main functional groups of the asphaltenes, like carbonyl, pyrrolic, pyridinic, sulphite, and thiophenic. Figure 9 shows a representative scheme of the asphaltene adsorption over nanoparticles

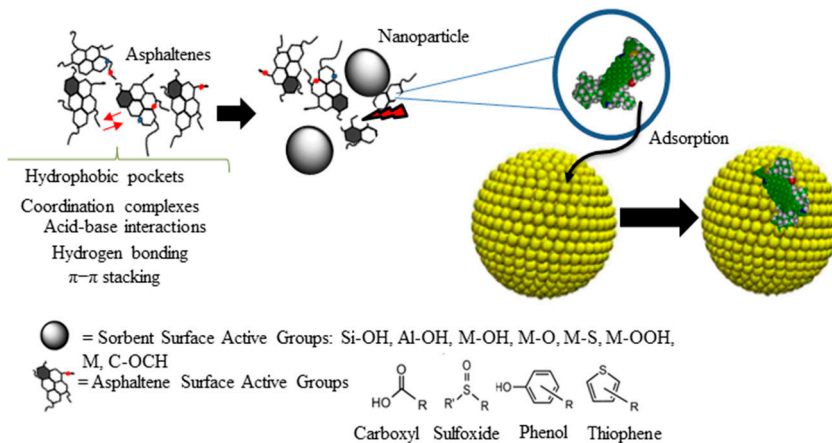


Figure 9. Asphaltene adsorption mechanism on nanoparticles. The interactions between the nanoparticles and the asphaltenes are favored by the functional groups present in the molecular structure of each one, depending on the nature of the nanoparticle, this will have active groups such as Si-OH, Al-OH, M-OH among others.

In a complement to the experimental studies, mathematically and computationally, studies have also been developed to understand the interactions between asphaltenes and nanoparticles, such as the solid-liquid equilibrium model (SLE) [109]. The model allows describing the adsorption isotherms of *n*-C₇ asphaltenes over different solid surfaces based on three parameters, namely, Henry's law constant (*H*), constant of *i*-mer reactions (*K*) and maximum amount adsorbed. Considering the first two variables, *H* indicates the adsorption affinity between the adsorbent-adsorbate couple, where the higher the *H* value, the lower the affinity. By contrast, *K* is an indicator of rapid association of asphaltenes once the primary sites over the nanoparticles are occupied [109]. Among the studies that evaluate the influence of asphaltene aggregation on asphaltene adsorption, Franco et al. [37] found through the use of heptol solutions in different ratios (Heptane-Toluene) that with the increase of heptane in the systems, higher adsorption affinities are obtained [37].

In the crude oil matrix, the interactions between asphaltene, resins and nanoparticles can lead to viscosity reduction and is mainly driven by the disruption of the viscoelastic network [92]. This mechanism is based on the disaggregation of the viscoelastic network formed by asphaltenes and resins within the fluid, through interactions between the functional groups of nanoparticles and asphaltenes, since these interactions are stronger than those that exist between asphaltene molecules [94]. Accordingly, several studies have demonstrated that nanoparticle addition of different chemical natures in HO and EHO generates a reduction in viscosity for low nanoparticle concentrations [92,93,110,111]. Comparative studies show that SiO₂ nanoparticles reduce the viscosity to a greater degree than Al₂O₃ and Fe₃O₄ nanoparticles of different sizes and degrees of surface acidity [112]. In addition, modification in the surface acidity of silica nanoparticle affects the interaction forces; and the performance of these will depend on the amount of active and basic sites of asphaltenes.

Figure 10 shows the rheological behavior of a HO in the presence of different nanoparticles at 25 °C between 0 and 75 s^{−1}. A similar trend is observed for all nanoparticles, reflected in the decrease in viscosity, and with a higher viscosity reduction degree for S8 nanoparticles. In general, when oil is subjected to deformation, and the magnitude of this increases, the microstructure formed by physical asphaltene bonds are destroyed. Then, the bonds weaken, and the asphaltenes move away from each other until they reach a point where a suspension is obtained. When the nanoparticles are added,

a similar tendency is observed. However, from the beginning of the adsorption of asphaltenes, the three-dimensional network is disorganized. With the increase in the shear rate, a decrease in viscosity occurs again, until it reaches a point where the magnitude of this value is independent of the shear rate [113].

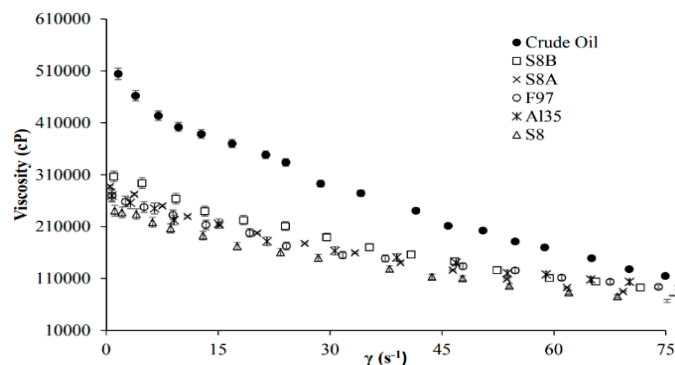


Figure 10. Viscosity as a function of shear rate in absence and presence of different nanoparticles such as basic silica of 8 nm (S8B), acidic silica of 8 nm (S8A), neutral silica of 8 nm (S8), alumina of 135 nm (Al35), and Fe_2O_3 of 97 nm (F97). Reprinted with permission [94]; Copyright 2017, Elsevier.

4. Influence of Nanoparticles in the Air Injection Process

Among the thermal enhanced oil recovery methods that use air injection in the reservoir are in-situ combustion (ISC) [114], Toe To-Heel Air injection (THAI) [115,116], and THAI/CAPRI [117,118] which uses a commercial catalyst around the horizontal producing well to accelerate the oxidation reactions, allowing a heavy crude to reach a gravity of 28° API [119,120]. In this context, the use of catalysts has received great attention from industry and researchers, in order to accelerate the reactions involved in these processes such as oxidation, catalytic disintegration, distillation, and polymerization, which contribute simultaneously with other mechanisms such as steam thrust and vaporization [121].

4.1. Metal and Metal Oxide Nanoparticles

Among the most studied materials are the metal oxide nanoparticles. It was found that the presence of NiO nanoparticles decreases the oxidation temperature of *n*-C₇ asphaltenes from 450 to 325 °C and the activation energy from 91 kJ·mol^{−1} for a temperature range between 467 and 514 °C to 57 kJ·mol^{−1} for temperatures between 280 and 350 °C [41]. Additionally, it has been found for NiO nanoparticles that a smaller particle size generates a greater catalytic effect as observed for the oxidation of quinolin-65 which is an asphaltene model molecule [122] and in the oxidation of *n*-C₅ asphaltenes [123]. Comparing the performance of NiO nanoparticles with other materials, Co₃O₄ nanoparticles also reduce the *n*-C₇ asphaltenes decomposition temperature to 325 °C. However, the intensity of the peak generated in the thermogravimetric analyses at this temperature is lower. In the case of the Fe₃O₄ nanoparticles, the main decomposition peak is generally found at 365 °C [41]. Regarding differential scanning calorimetry studies (DSC), when asphaltenes are adsorbed on the nanoparticles, the combustion and oxidation occur at lower temperatures. In the absence of nanoparticles, an exothermic effect is observed from 450 °C, whereas when they are adsorbed onto NiO, Fe₃O₄, and Co₃O₄ the heat flow evolved drastically. Variations in iron-based nanoparticles, such as maghemite (γ -Fe₂O₃), showed that the starting temperature of the asphaltene oxidation and the temperature of the maximum oxidation rate decrease by 203 and 123 °C, respectively [124].

In the case of copper nanoparticles, its effect on the combustion process was evaluated by measuring the oxidation kinetics of crude oil, observing an improvement in the rate of combustion at a concentration of 1000 mg·L^{−1} of nanoparticles. The Cu-NP also allows inhibiting the oxidation reactions at low temperatures, which prevents the increase of the crude oil viscosity in the combustion front [53]. Additionally, hydrophobic CuO nanoparticles increase the average rate of oxygen consumption

1.4 times compared to the experiment without nanoparticles, at low temperatures (LTO), which translates into a reduction in the residual oxygen content [39]. Using high pressure differential scanning calorimetry (HP-DSC) and accelerating rate calorimetry (ARC) it was demonstrated that this nanomaterial significantly improves the oxidation performance of crude oil through the reduction of induction time, reduction of ignition temperature, decrease in activation energy values, and improvement of coke combustion efficiency, both at low and high temperatures [125].

4.2. SiO₂ and SiO₂-Based Nanoparticles

The effect of SiO₂ nanoparticles (amorphous, fumaric, crystalline, commercial, and functionalized) on the asphaltene decomposition under oxidative conditions has been widely studied. Through the change in the surface acidity of the silica nanoparticles, it was demonstrated that catalytic activity is strongly dependent on the surface acidity nature of the catalysts [40]. The temperature increased in the following order basic < neutral < acid < virgin asphaltenes. In addition, the basic and acid nanoparticles promoted the production of CO and CH₄ over other gases. The use of silica nanoparticles as support for low loadings of nickel and/or palladium oxides improves the catalytic efficiency of the nanoparticles. It has been found a higher catalytic activity of bimetallic samples in comparison with monometallic samples. A synergistic effect between bimetallic nanoparticles and support reduces the oxidation rate of asphaltenes at even lower temperatures (<300 °C) [82]. Figure 11 shows a scheme of oxidative reaction and the asphaltene oxidation temperature under oxidation conditions obtained by several nanomaterials. Clearly, the figure shows that the functionalization of support generates better catalytic performance. In this sense, the SNI1Pd1 exhibits the lower asphaltene decomposition temperature and CO₂, H₂O, NO_x, and SO_x among others are generated as products of the reaction.

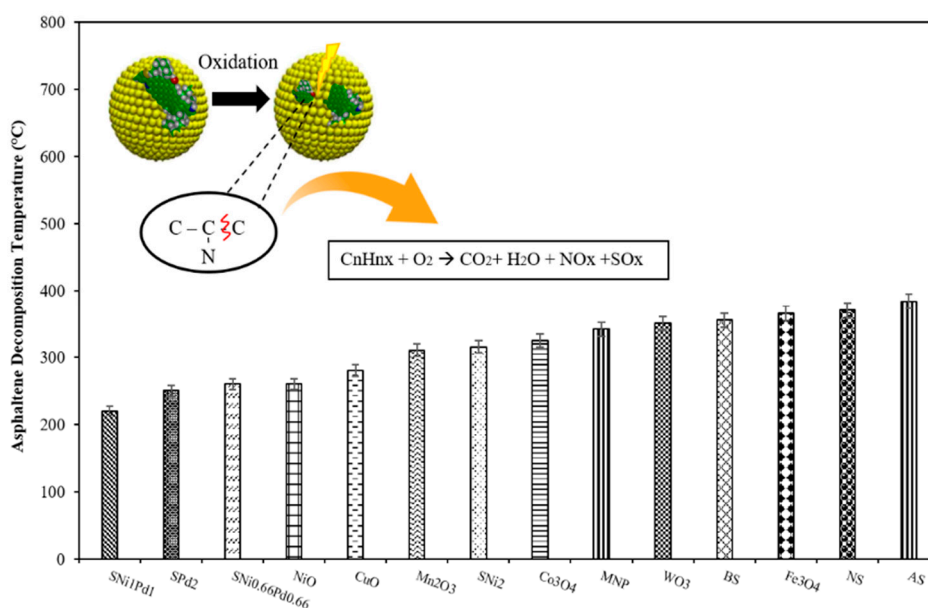


Figure 11. Scheme of oxidative reaction and asphaltene oxidation under air atmosphere obtained by several nanomaterials. SiO₂ nanoparticles functionalized with a mass fraction of 1% of NiO and PdO (SNI1Pd1), with 0.66% of NiO and PdO (SNI0.66Pd0.66), with 2% of NiO (SNI2) with 2% of PdO (SPd2), basic silica (BS), neutral silica (NS), acidic silica (AS), and others.

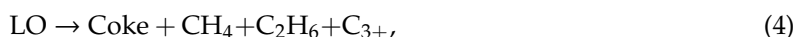
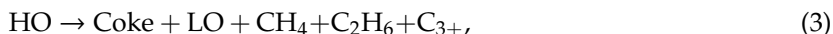
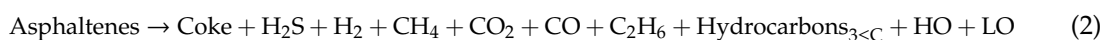
Other studies have evaluated the influence of other factors on the oxidative decomposition of asphaltenes. In general, in the absence of nanoparticles, resins I had no significant effect on the *n*-C₇ asphaltenes oxidation under air atmosphere. However, in the presence of SNI1Pd1 NPs, the oxidation temperature of *n*-C₇ asphaltenes dramatically decreases up to 250, 260, and 270 °C for a load of resins 0.20, 0.10, and 0.06 mg·m⁻², respectively. Besides, the activation energy presented a similar behavior

that at higher content of adsorbed resins, the activation energy was lower [73]. On the other hand, the asphaltene loading on the surface of the nanoparticle modifies the efficiency of the oxidation process [37]. While the load of asphaltenes decreases, the temperature to generate the same degree of conversion thereof decreases, i.e., the degree of conversion increases, due to a greater provision of active sites in the nanoparticle for the reaction [37]. In addition, the influence of asphaltene aggregation over the catalytic oxidation performance of fumed silica and NiO- and PdO- supported on fumed silica nanoparticles was evaluated by asphaltene adsorption over systems with mixtures of toluene and heptane. The authors demonstrated that catalytic activity of the nanoparticles is affected by this phenomenon since a higher aggregation degree of the asphaltenes decreases the catalytic activity of the nanoparticles, which is reflected in the increase in activation energy values and the decrease in CO₂ and CO production [37].

Finally, it is important to mention that to date there have been no studies under dynamic conditions of the air injection processes, opening the opportunity for a deeper investigation in this regard to better understand the background implications that oxidation reactions have on the decomposition of heavy crude oil fractions.

5. Influence of Nanoparticles in Steam Injection Processes

Among the methods of enhanced oil recovery, there is a wide range of processes that take advantage of the thermal properties of steam to generate the decomposition of heavy molecules through gasification, methanation, steam reforming, hydrogenation, aquathermolysis, and water-gas shift reactions [47]. The aquathermolysis reactions begin with the cleavage of the bonds C-S present in the molecular structure of the *n*-C₇ asphaltenes, generating the production of H₂S, because C-S bonds are the bonds with smaller energy of dissociation [126]. The reaction mechanism is shown below



where, LO is light oil and HO is heavy crude oil. In this way, there is a decrease in the heavy fraction content in the crude oil matrix and as a result of these reactions, the H/C ratio increases, the quality of the crude oil improves, and the viscosity thereof decreases.

Among the most used techniques are continuous steam injection [127], cyclic steam stimulation (CSS) [128], and steam-assisted gravity drainage (SAGD) [2]. Steam injection techniques do not provide recovery factors greater than 50% [32,49], therefore the industry is looking for techniques to improve the performance of these processes. In this sense, these techniques in combination with nanotechnology have emerged with the main challenge of reducing the asphaltene decomposition temperature and improve the oil recovery. Figure 12 shows a step-by-step diagram of a catalytic steam gasification process. In a first step the asphaltenes are adsorbed on the nanoparticles generating the viscosity reduction by the disaggregation of the viscoelastic network. Subsequently, the asphaltene decomposition by effect of catalytic steam gasification process is carried out. Finally, CO₂, H₂, CO, and CH₄ products are generally obtained in the gasification of heavy hydrocarbons.

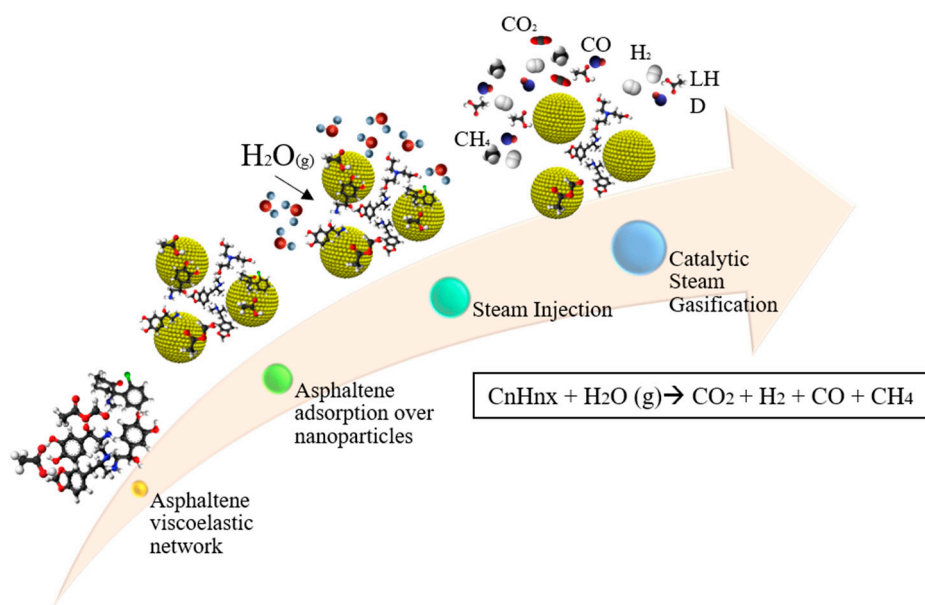


Figure 12. Basic scheme of the gasification process of asphaltenes in the presence of nanoparticles. Several steps are shown, (i) asphaltene viscoelastic network followed by the (ii) asphaltene adsorption on nanoparticles generating the viscosity reduction by the disaggregation of the viscoelastic network. (iii) Steam injection and (iv) asphaltene decomposition by effect of catalytic steam gasification process assisted by nanoparticles. The equation refers to the products generally obtained in the gasification of heavy hydrocarbons.

5.1. Metal Oxide Nanoparticles

Several studies propose the use of metal oxide nanoparticles for the enhancement of heavy and extra-heavy crude oil properties through interactions with the asphaltenes [45,88,129,130]. Thanks to the catalytic properties of the NiO nanoparticles, several technical approaches and particularly steam gasification reactions [24] have been carried out. Among the best results of the applications of these nanoparticles, is the reduction of the decomposition temperature of Athabasca asphaltenes from 500 to 317 °C in the steam presence [131]. Other studies compare the catalytic activity of NiO nanoparticles with other metal oxides such as Fe₃O₄ and Co₃O₄. In general, a decrease in the reaction temperature is observed from 500 to 380, 330, and 317 °C for Fe₃O₄, Co₃O₄, and NiO, respectively [131]. Studies on the application of nickel nanoparticles and industrial Raney nickel on steam-stimulation experiments have established important aspect as (i) the degree of in-situ upgrading is strongly dependent on the metal concentration, (ii) a higher degree of catalytic activity is associated to a higher surface-to-volume ratio, (iii) homogeneous distribution of the particles in the porous medium generates a higher efficiency of the upgrading [132].

5.2. Composite Materials

The use of different nanoparticles as catalysts improves the decomposition conditions of asphaltenes through gasification and hydrothermolysis reactions, besides inhibiting the addition reactions of this heavy fraction, by decreasing the peak intensity of decomposition in the high-temperature region (>500 °C). Functionalized nanomaterials have also been used for asphaltene gasification processes, in order to take advantage of the synergistic effect between the materials that make up the catalyst. SiO₂ [84], Al₂O₃ [87], CeO₂ [51], and TiO₂ nanoparticles [45] have been used as supports for metal oxide nanoparticles. In particular, functionalized SiO₂ with a mass fraction of 1% of Ni and 1% of Pd, generates an increase in the production of CH₄ over other gases in the steam gasification of asphaltenes [84]. Al₂O₃ nanoparticles functionalized with a mass fraction of 2% of NiO reduced the decomposition temperature approximately 100 °C and promoted the production of gases

such as CH₄ and CO above others such as CO₂, with a coke yield of approximately 0.13%. However, a mass fraction of 2% NiO supported on TiO₂ reduced the temperature by approximately 170 °C and starts the production of the same gases at a lower temperature although the coke residue is higher with a mass fraction of 0.17% [45].

Finally, in order to take these studies to a possible industrial application, the use of the catalysts in the catalytic steam gasification of Athabasca visbroken residue in a fixed-bed reactor was evaluated [129]. The possibility of gasifying this fraction successfully at low temperatures for its hydrogenation was demonstrated.

On the other hand, Ni-Pd/CeO₂ generates 93% of *n*-C₇ asphaltenes conversion that are absorbed under a steam atmosphere in a time less than 90 min. Finally, Ni-Pd/TiO₂ and Ni-Pd/Al₂O₃ reached decomposition temperatures of *n*-C₇ asphaltenes of 251 and 257 °C, respectively [45]. Janus-type nanoparticles have also been studied, which present a better scenario to improve the HO and EHO steam injection processes, since they lower the decomposition temperature of asphaltenes up to 200 °C [104]. In addition, these NPs alter other variables such as interfacial tension, whose value decreases due to the surface modification to which this type of material is subjected. In another study Core-Shell nanoparticles have been implemented [133]. In this sense, nanoparticles of silica shell-magnetite core have demonstrated to be efficient systems on the *n*-C₇ asphaltene decomposition under the steam presence. The decomposition over the nanocomposite starts at 200 °C, and the main peak occurs at 440 °C, 20 °C less than the temperature in which asphaltenes in the absence of nanoparticles are decomposed. Besides, the implementation of core-shell nanoparticles promotes the CH₄, CO, and light hydrocarbons produced during the decomposition of heavy oil fractions [13]. Besides, due to their magnetic properties, these nanoparticles could be recovered and reused in new injections, generating positive economic and environmental impacts [13,134].

The use of MoS₂ NPs doped with various modifications of Ni and thus effect of the content of this metal on the catalytic activity of the material was evaluated. For a ratio (Ni/Mo = 0.45) the best catalytic performance was found in hydrographic reactions in the improvement of crude oils.

As gasification processes involve a range of reactions giving as a result gases such as H₂, CO, CO₂, and CH₄, some studies have focused on catalytically improving certain specific reactions [135]. From the steam reforming, the amount of tar and hydrogen produced from bituminous oil was investigated. In general, with the increase in temperature, the conversion of tar into gas increases and, therefore, the amount of hydrogen increases [136]. When applying nanoparticles of Ni/Al₂O₃, Ni/Olivine, Ni/Fe₂O₃, the elimination of the tars is achieved in 99%, 93.1%, and 83.6%, respectively, at a temperature of 900 °C. The water gas shift reaction (WGS) has also been studied by using nanocatalysts based on cerium oxide (CeO₂) functionalized with different transition elements oxide (Fe, Ni, Co, and/or Pd) [88]. Here it was obtained an increase of the production of gases and light hydrocarbons facilitating the hydrogenation of asphaltene molecules due to three catalytic routes that involve the effect of the (a) interactions between metals and CeO₂, (b) the redox cycle of the support, and (c) the production of hydrogen under two mechanisms that govern the WGSR: redox and formates. Systems compounds by a fraction mass of 1% of Fe-Pd, Co-Pd, and Ni-Pd were employed to estimate the catalytic activity of the nanomaterials to carry out gasification reactions at low temperatures below 240 °C. A really good performance for the couple Ni-Pd supported in CeO₂ nanoparticles was obtained, and it is directly related to the influence of nickel oxide as a dispersion material, the beneficial effect of palladium oxide and cerium oxide as an active support material to accelerate the gasification reactions [51]. In this sense, statistical designs to improve the efficiency of gasification processes have been employed (Figure 13). Simplex-centroid mixture design was used to optimize the mass fraction % of NiO and PdO over CeO₂ nanoparticle surfaces, and it was found that with a mass fraction of 0.89 and 1.1 of PdO and NiO, respectively, the asphaltene conversion was maximized at 100% in less than 80 min.

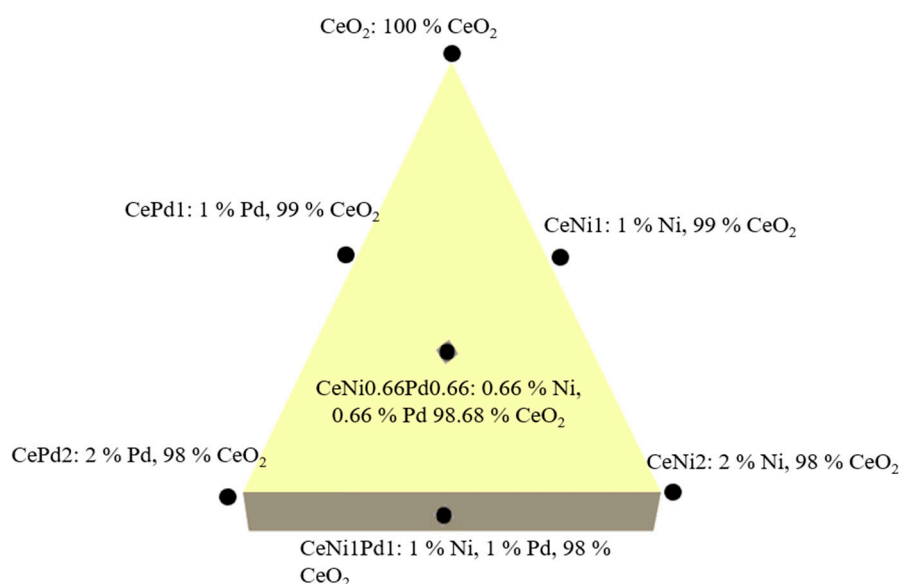


Figure 13. Three components simplex-centroid mixture design with ceria support (CeO_2) functionalized with nickel oxide (NiO) and palladium oxide (PdO). Reprinted with permission [88]; Copyright 2019, MDPI.

From the catalytic evaluation of the seven nanoparticles with the concentrations suggested by the statistical design, the optimum concentration of these metals on the surface of the nanoparticle was determined. Additionally, through the samples used, an increase in the catalytic activity of the bimetallic nanoparticles was observed with respect to the monometallic ones, and a greater effect of the Pd than Ni oxides. Thus, the conversion increased in the order $\text{CeO}_2 < \text{CeNi1} < \text{CePd1} < \text{CeNi2} < \text{CeNi0.66Pd0.66} < \text{CePd2} < \text{CeNi1Pd1} < \text{CeNi0.89Pd1.1}$. On the other hand, the self-regenerative property of ceria nanoparticles functionalized with the optimal load of the metal oxides of Ni and Pd was evaluated in their adsorptive and catalytic performance for asphaltene steam gasification. In this sense, nine catalytic cycles were studied, and it was found that the affinity of the asphaltene for being adsorbed over the nanoparticles remains strong with the passage of the cycles, reflected on the type I behavior of the adsorption isotherms, and the decrease in around a 2.6% of Polanyi's adsorption potential. In addition, the catalytic activity of the nanoparticles is not affected by their regeneration, because they are able to decompose 100% of the amount adsorbed in the nine cycles, and the activation energy only increases by $49.1 \text{ kJ}\cdot\text{mol}^{-1}$ units [51]. All these studies give account of the catalytic phenomena that occurred thanks to the effect of the nanoparticles with the asphaltenes at static conditions, however for a more approximate study to reservoir conditions, nanoparticles of silica, alumina, functionalized silica [49], ceria functionalized with NiO and PdO [51], and functionalized alumina [87] have been evaluated at high-pressure conditions. For ceria nanoparticles it was obtained an increase in recovery factor from 63.5% to 75.3% in steam injection with a quality of 70% and 240°C , highlighting that a hydrogen donor agent was not used to perform the displacement test. In addition, the crude oil quality experienced a great upgrade. In fact, asphaltene content was reduced from 28.7% to 12.9%, API gravity increased by approximately a 50%, and the viscosity reduction was around 78%. All these results are explained by two main mechanisms, where viscosity reduction is caused by a re-organization of the crude oil viscoelastic network by the strong interactions between asphaltene and nanoparticles that are generated and by the catalytic activity of the nanoparticles.

For monometallic and bimetallic nanoparticles supported on Al_2O_3 nanoparticles, in the first instance, it was demonstrated that the variation of steam quality in the absence of nanoparticles generates an impact on the oil recovery factor (RF), showing a higher value for the RF for a higher steam quality, however, the quality of the crude does not change. With the addition of nanoparticles,

an increase in °API gravity of approximately 5 and 7° API was achieved for the AlNi₂ and AlPd1Ni1 nanoparticles, respectively, so there was a permanent improvement in oil quality, including an increase in recovery for a quality value of 50% of 20% and 13% for the use of bimetallic and monometallic nanoparticles, as shown in Figure 14.

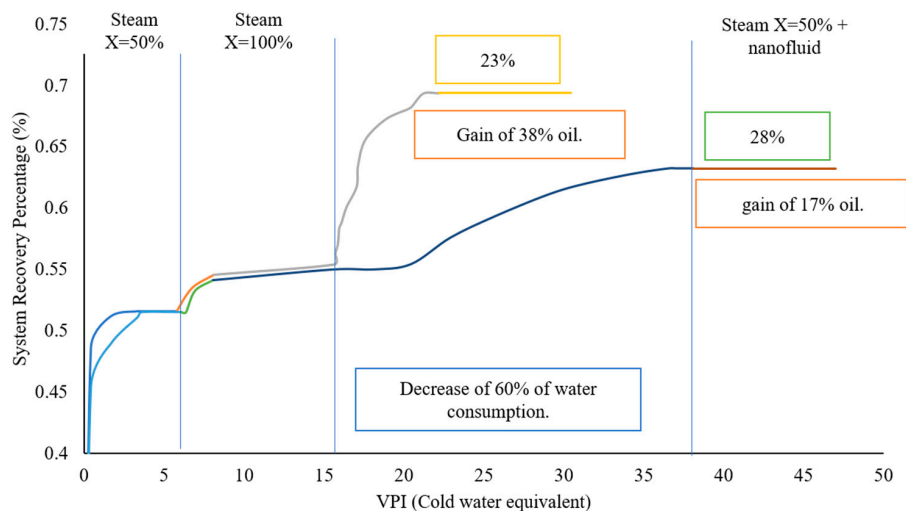


Figure 14. Effect of steam quality ($X = 50\%$ or 100%) in recovery factor for steam injection process in the presence of nanofluid with monometallic and bimetallic nanoparticles. Recovery factor curve reprinted with permission [87]; Copyright 2018, Universidad Nacional de Colombia.

On the other hand, another study involved the use of nanofluids of SiO₂ nanoparticles functionalized with nickel and palladium oxide at a mass fraction of 1% (SiNi1Pd1) and a recovery of 56% was observed. Additionally, under these same conditions and fluids, the characterization of the effluents after the steam injection shows an increase in the API gravity of the crude from 7.2 to 12.1°. In addition, through SARA analysis and simulated distillation (SimDis), it was demonstrated that the asphaltene content had decreased in the oil crude matrix (Figure 15) and that the viscosity of the fluid had increased [49].

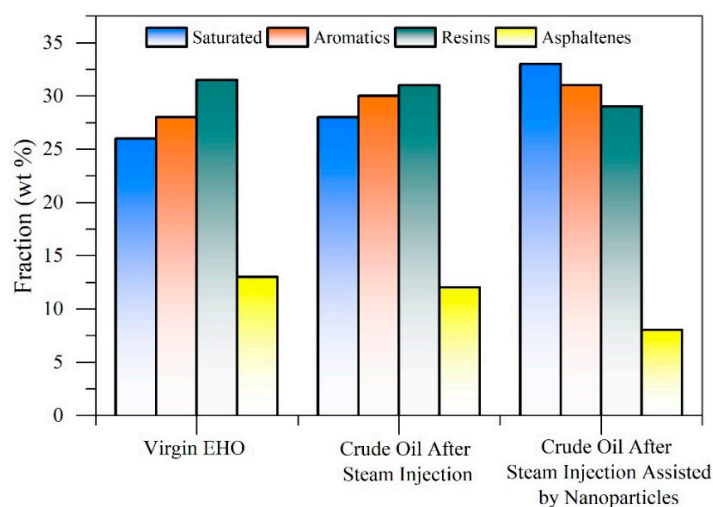


Figure 15. Saturates, aromatics, resins, and asphaltene content analysis of an extra-heavy crude oil before and after recovery with steam injection in the presence and absence of 1000 mg·L⁻¹ of SiNi1Pd1 nanoparticles. Injection pressure and temperature were maintained at 8.96 MPa and 300 °C, respectively. Reprinted with permission [49]; Copyright 2018, MDPI.

Another important result obtained with the application of SiNi1Pd1 nanoparticles is the reduction in viscosity and the shift in rheological behavior of the heavy crude oil, which has a Newtonian behavior after being in contact with the steam and the nanocatalyst. It implies that viscosity reduction can be enhanced at both surface and subsurface conditions. Figure 16 shows the rheological behavior at 25 °C for the three scenarios: virgin heavy crude oil, heavy crude oil after steam injection, and heavy crude oil after steam injection assisted by nanoparticles.

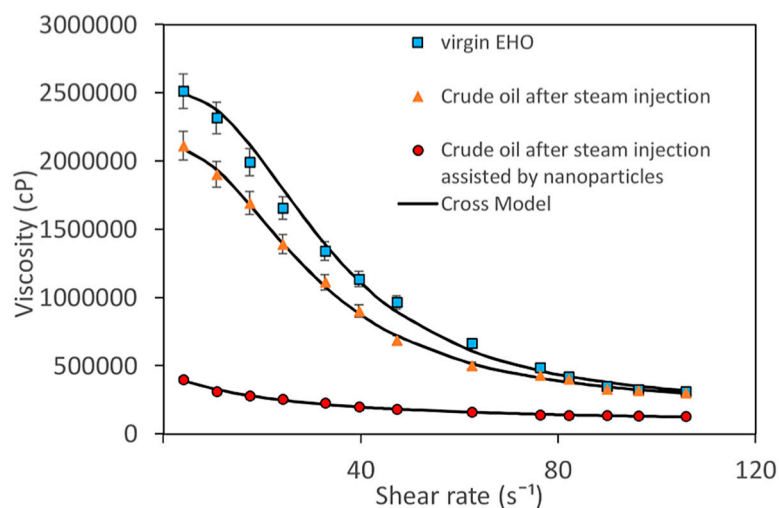


Figure 16. Rheological behavior of an extra-heavy crude oil in the presence and absence of steam assisted and nonassisted by 1000 mg·L⁻¹ of SiNi1Pd1 nanoparticles. Operation conditions was fixed at 8.96 MPa and 300 °C. The points are the experimental data and the continuous line refers to the Cross model. Reprinted with permission [49]; Copyright 2018, MDPI.

Besides, trimetallic nanoparticles of Ni, W, and Mo were dispersed in vacuum oil gas to perform an steam-assisted gravity drainage (SAGD) test, for a temperature range of 320–340 °C [137]. The catalytic activity of the nanomaterial promotes a decrease in sulfur- and nitrogen-based gas production, reducing the emission of greenhouse gases, and producing valuable end products. In the case of Cyclic Steam Stimulation (CSS), it was simulated at 240 °C, using a silica sand pack doped with nickel nanoparticles. The recovery factor increases by 10% respect to the scenario in the absence of the nanoparticles [138]. In addition, the same process was simulated to evaluate the influence of the nanoparticles for promoting aquathermolysis reactions between 150 and 220 °C. In this particular experiment, the nanoparticles were mixed with the heavy oil before the start of the process. An incremental in 14% for oil recovery factor was reached at 220 °C [24].

6. Influence of Nanoparticles in Pyrolysis Reactions

Within the processes of asphaltenes decomposition, both in processes involving the air or steam injection, there is the possibility of chemical interactions occurring between the products of pyrolysis reactions such as coke. Pyrolysis or thermolysis is basically the thermochemical decomposition of the crude oil components at elevated temperatures in the absence of oxygen [139]. Early studies showed that thanks to thermal cracking, the crude oil recovery was improved because the elevated temperatures at which this reaction occurs allows a change in the C/H ratio, a reduction in the content of nitrogen and sulfur [140]. The oil produced had a high reduction in the asphaltene content and an increase in saturates. The gas was mainly composed of hydrogen, methane, and ethane. In this order of ideas, from the bitumen, gas, coke, and oil are generated as main products [140]. Due the high temperatures of this reaction, implementing nanocatalysts to reduce the temperature and enhance the crude oil under the thermal cracking of its heavy fractions has recently been studied.

The performance of three transition metal oxides NiO, Co_3O_4 , Fe_3O_4 has been compared in the pyrolysis of asphaltenes under inert conditions [44]. In terms of thermal cracking temperature reduction of asphaltenes and the energy needed to activate the thermolysis reactions, a better performance was carried out by the NiO nanoparticles followed by Co_3O_4 and Fe_3O_4 [44]. Besides, the study reported that during the pyrolysis of asphaltenes, the C-S bonds are broken around 350–400 °C, while the C-C bonds require temperatures higher than 400 °C, which are relatively elevated temperatures, and for which the use of a catalyst is necessary, with which, these temperatures are reduced to approximately 250–300 °C. Asphaltenes from Maya crude oil were subjected to pyrolysis, obtaining maltenes, gases, and coke as products [141]. This is explained by the fact that heterocyclic nitrogen can play a key role in the thermal cracking reactions of asphaltenes and resins, since the first reactions involve the breaking of aromatic alkyl bonds. On the other hand, secondary reactions involve the condensation of aromatic rings and the aromatization of naphthenes. According to this, the first step for the formation of coke from the heavier fractions of the crude matrix is the obtaining of volatile hydrocarbons [142].

In addition, for ex-situ- and in-situ-prepared NiO nanoparticles, the coke residue of pyrolysis and post-pyrolysis was investigated through temperature-programmed pyrolysis (TPP) and temperature-programmed oxidation (TPO), and it was demonstrated that in-situ NiO nanoparticles, compared to the ex-situ NiO, modify the oxidation temperature by approximately 100 °C below the initial one for the free coke, this added to a significant reduction in the activation energy. These results are corroborated with the conversion (α) of the free coke, in-situ prepared coked NiO and ex-situ prepared coked NiO after the TPP test at three different heating rates, and in all cases, the temperature necessary to convert the same fraction follow the order free coke > coked ex-situ NiO > coked in-situ NiO. Figure 17 shows the relationship between the activation energy and temperature/conversion.

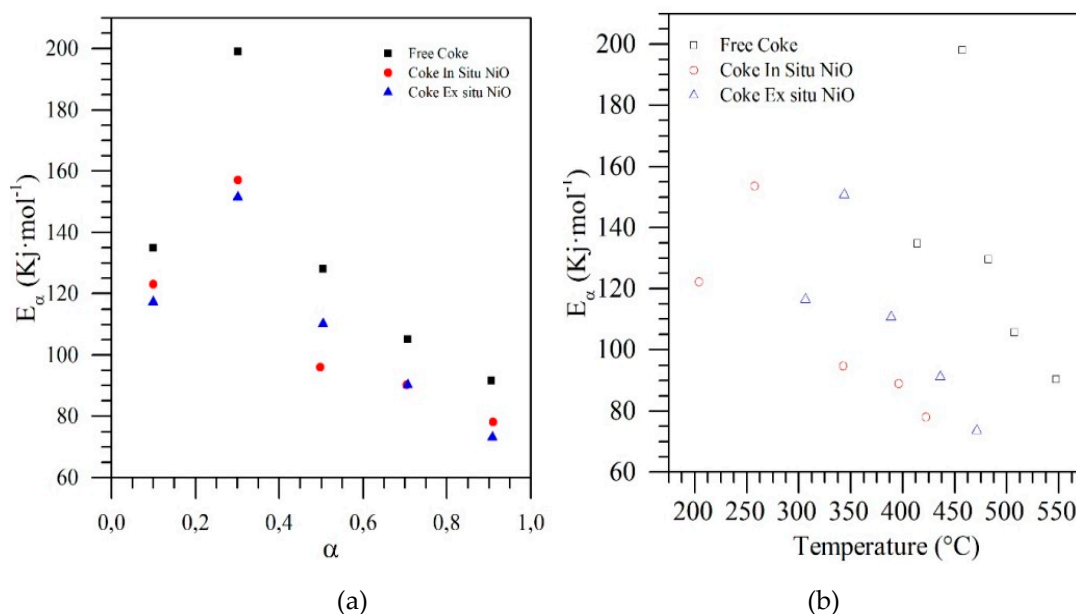


Figure 17. Relationship between activation energy (E_α) with (a) conversion degree (α) and (b) temperature for thermo-oxidative decomposition of post-temperature-programmed pyrolysis (TPP) samples in the presence and absence of NiO nanoparticles in-situ and ex-situ. Reprinted with permission [38]; Copyright 2018, ACS Publications.

Figure 17 confirms the greater catalytic effect of the coke over in-situ nanoparticles NiO, because coke decomposition reactions start at lower temperatures, compared to ex-situ nanoparticles, and without nanoparticles. Additionally, the energy needed to generate the same degree of conversion decreases for the presence of nanoparticles (Figure 17b). For example, to convert 50%, the activation energy follows the order in-situ < ex-situ < free coke.

Different nanomaterials have been applied to study the pyrolysis of asphaltenes, its oxidation after the pyrolysis of the coke formed. NiO nanoparticles can improve the efficiency of both processes including influencing the oil production in situ of the reservoir [42]. Silica and magnetite nanoparticles increase the amount of fuel produced at low and high temperatures under oxidation and pyrolysis reactions. These nanoparticles achieve a reduction of the activation energy by increasing the production of crude oil [143]. The experimental data suggest that the thermal cracking of asphaltenes and resins to coke is a complex process in which the following reactions take place: (a) cracking of alkyl chains of aromatic groups, (b) dehydrogenation of naphthenes to form aromatic compounds, (c) condensation of aromatics to higher fused ring aromatic compounds, and (d) dimerization/oligomerization reactions. The loss of alkyl chains always accompanies thermal cracking and the dehydrogenation/condensation reactions are a consequence of hydrogen deficient conditions. These results reflect the catalytic capacity of nanoparticles that vary from transition metals, metal oxides, and even organic base, achieving improved efficiency of oxidation, gasification, pyrolysis reactions individually or combined allowing the upgrading of heavy and extra-heavy crude oils through of the decomposition of asphaltenes.

7. Influence of Nanoparticles on Electromagnetic Heating for Heavy Crude Oil

The radiation heating for the recovery of heavy crude oil is divided into distinct categories depending on the type of frequency of the electric current used to generate the heating [144]. For low frequencies, heating by resistance or ohmic is given, while the induced heating, on the other hand, induces a secondary current to produce heat, and for high frequencies (microwave) the way to generate heat is due to the molecules forming dipoles and they align them in an electric field. The electrical current is induced by a coil located in the injector well, and in general, it is recommended to use two horizontal wells like the SAGD technique [145]. Since most conventional methods do not resist processes involving high pressures and high temperatures (HTHP), the application of electromagnetic energy has been chosen in conjunction with the application of nanotechnology. During a study, a noninvasive method was evaluated in order to inject magnetic irradiation into the reservoir in conjunction with a dielectric nanofluid, this in order to increase oil production through perturbations in the water/oil interface [146]. The study showed that the presence of magnetic nanoparticles compared to commercial surfactant (SDS) increases the recovery factor in the absence of EM and with the irradiation of these waves, the recovery of residual oil increased even more.

In addition, a key factor was the viscosity of the dielectric nanofluids which allows improving the sweeping efficiency and therefore the amount of oil recovered [146]. Due to the ability to absorb microwaves, metal oxide nanoparticles have been widely studied for the improvement of heavy crude oils by increasing the temperature of the system. Oxides of iron, nickel, and copper were used experimentally in microwave heating and obtained a viscosity reduction of up to 20% for nickel NPs which showed the best performance at lower microwave powers [147].

Copper oxide and nickel oxide nanoparticles of 50 nm enhance the oil recovery in low permeability carbonates, giving as main results an oil recovery by 9%–22% over the recovery by other conventional methods like waterflooding. Between copper (II) oxide (CuO), nickel oxide (II), and iron (III) oxide, NiO nanoparticles increase the recovery factor (85%) above the other two nanoparticles due to the fact that these nanoparticles are less conductive and therefore travel more slowly than CuO and Fe₂O₃. Cobalt ferrite nanoparticles (CoFe₂O₃) have also been used to improve this technique. These nanoparticles of 51.17 nm are injected into a glass beads sample in the PVC column under the scheme shown in Figure 18 [148].

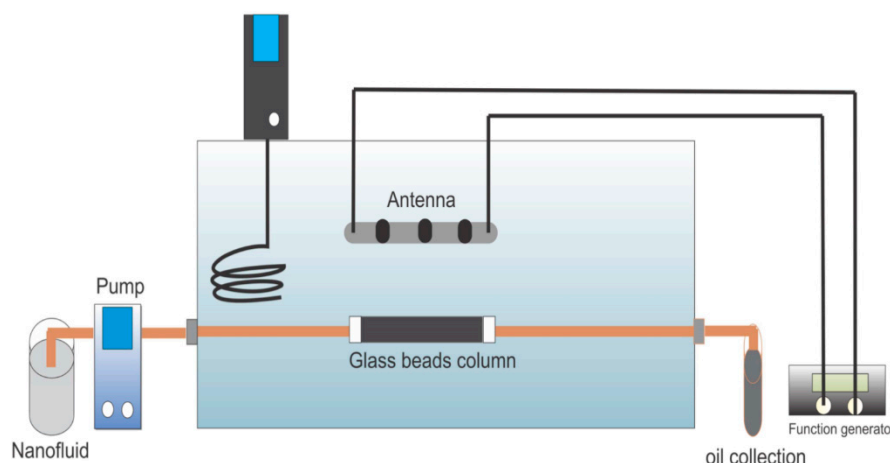


Figure 18. Schematic diagram of the experimental setup for nanofluid enhanced recovery oil (EOR). Reprinted with permission [148]; Copyright 2012, Trans Tech Publications Ltd.

The nanoparticles are pumped into the glass bed while being exposed to EM waves for 24 h through a generator function. Finally, the recovery factor is calculated, and its results are shown in Table 2.

Table 2. Enhanced oil recovery after nanofluid injection in the absence and presence of electromagnetic waves. Adapted with permission [148]; Copyright 2012, Trans Tech Publications Ltd.

Stage	Original Oil in Place (mL)	Volume of Oil Recovered after Water Flooding (mL)	Residual Oil in Place after Water Flooding (mL)	Oil Recovered after Nanofluid Injection (mL)	Percentage Recovery Factor (%)
Nanofluid injection	46.0	34.5	11.5	1.0	8.7
Nanofluid injection with electromagnetic waver	42.5	33.0	9.5	3.0	31.6

Iron nanopowder, iron oxide, and iron chloride were used to evaluate de viscosity reduction, and due to the strong attraction for asphaltenes the iron nanopowder achieves a significant reduction in viscosity with respect to the other two [149]. In addition, varying the concentration of the nanopowder, it was found that there is a critical concentration of nanoparticles that generates the greatest efficiency in viscosity reduction [111,150].

Finally, another application reported thanks to the effect of reducing the speed of the electromagnetic waves when crossing magnetic media (higher magnetic permeability), allows a mapping inside the reservoir by locating magnetic nanoparticles inside the injected fluids and in this way mapping its flood front and movement of fluids [146,151].

8. Implementation Plan of Nanotechnology for the Steam Injection Process

Applications of nanotechnology in EOR has not had much attention in the past due to inadequate understanding of the mechanism, high chemical costs, and low crude oil prices. However, a complete plan implementation will allow the exploitation of recent advances in nanotechnology, being a novel and cost-efficient alternative. It is necessary to develop a technology implementation plan that provides better results in pilot tests for the subsequent expansion and the successful application of nanoparticles in thermal enhanced oil recovery processes. This plan aims to provide selection criteria reducing the risks and uncertainties associated with conventional technology and application of nanotechnology as a means to improve the process, considering the critical parameters in the performance and technical limits. The methodology to carry out the implementation plan could be divided into three principal stages of work. These are (1) experimental evaluation, (2) reservoir characterization and engineering, and (3) management of surface facilities. The experimental evaluation will allow to determinate the phenomena that occur when executing the nanotechnology at well scale. Information about the efficiency of the process through the use of nanotechnology is obtained through different tests. Thus, the type of tests can be classified into two main groups, static tests and dynamic tests [29,30,32,33,38,41,45,82,152,153]. In the reservoir characterization and engineering stages, it is of primary importance to analyze the characteristics and dynamics of production of the field in order to determine the viability of the steam injection technology through the use of nanofluids. Different properties and characteristics such as viscosity, API gravity, permeability, porosity, pressure, and oil saturation should be evaluated. This stage provides important information for making predictions, evaluating various development plans that allow defining the best scenario to recover the hydrocarbons present in the reservoir. Moreover, the information necessary to carry out a methodology for the selection of the well or the most appropriate pilot area where the enhanced thermal recovery method can be implemented by using nanotechnology is obtained. The third stage will allow guaranteeing the optimal and safe operation of the surface facilities during the operations of production, separation, storage, and injection of fluids a strategic plan to dispose and control the fluids produced is realized. This includes knowledge about fluid, regulations and nanoparticle disposition, monitoring of the nanoparticles, control, and quality of water, design of surface facilities, among others.

9. Environmental Impacts

According to the literature, catalytic nanoparticles for in situ heavy oil upgrading have demonstrated a reduction in costs and positive environmental impacts [154,155]. Among the advantages that offer the use of NPs in thermal oil recovery processes are (1) decreasing heat consumption, the NPs in contact with oil molecules accelerate the cracking and hydrogenation of hydrocarbons, generating more heat and gaseous products that further improve the oil detachment from the rock. Therefore, the introduction of NPs to catalyze the chemical reactions generate a reduction of the heat consumption [54]; (2) sulfur removal, to meet the strict environmental regulations on hydrocarbons transportation [156]. Several authors have demonstrated a marked sulfur removal effect evidencing the effectiveness of NPs application for enhanced upgrading and better product quality [92,132,157,158]; (3) reduction of water consuming, ZnO₂ nanoparticles have shown a reduction of viscosity and increases heavy crude oil recovery whereas WCUT% is decreased through the SAGD process [159]; (4) reduction of toxic chemical and capital cost of lifting operation and transportation from downhole to refinery center. The main techniques that exist for the OH and EHO transportation require the addition of solvents (light crude oil, naphtha, diesel, among others) or gases (mainly, CO₂), as they contribute to reducing oil viscosity [160–163]. High consumption of solvents increases transportation costs and generates different environmental risks due to the production of polluting gases. It has been demonstrated that addition of 10% of nanofluids prepared with biodiesel and 1000 mg·L⁻¹ of SiO₂ nanoparticles can reduce the naphtha by more than 50% [92]; (5) reduction of greenhouse gases, CO₂ leakage prevention mechanisms through nanoparticle application have been reported. The study evidenced a remediation strategy by effect of injection of nanoparticle dispersion into a leakage

pathway after CO₂ escape [164]. (6) Environmental remediation technology nanoparticles represent a new generation of environmental remediation technologies that could help solve some of the most challenging environmental problems [165–167]; (7) reduction of technology costs since NPs can be cheaper than chemicals, for example, it has been reported that silica nanoparticles (SiNPs) improve oil production being environmentally friendly since are the main component of sandstone [143,168]. SiNPs are cheap and their chemical behavior could be easily controlled by surface modification [168]. Figure 19 shows an example of (a) sulfur reduction in the presence of nanocatalysts and (b) reduction of naphtha consumption. All advantages mentioned make evident that nanoparticles applied in EOR processes have the ability to improve oil production being environmentally friendly, less expensive, and more efficient compared to traditional chemicals. By this reason, the intensive search of nanomaterials to EOR processes is needed.

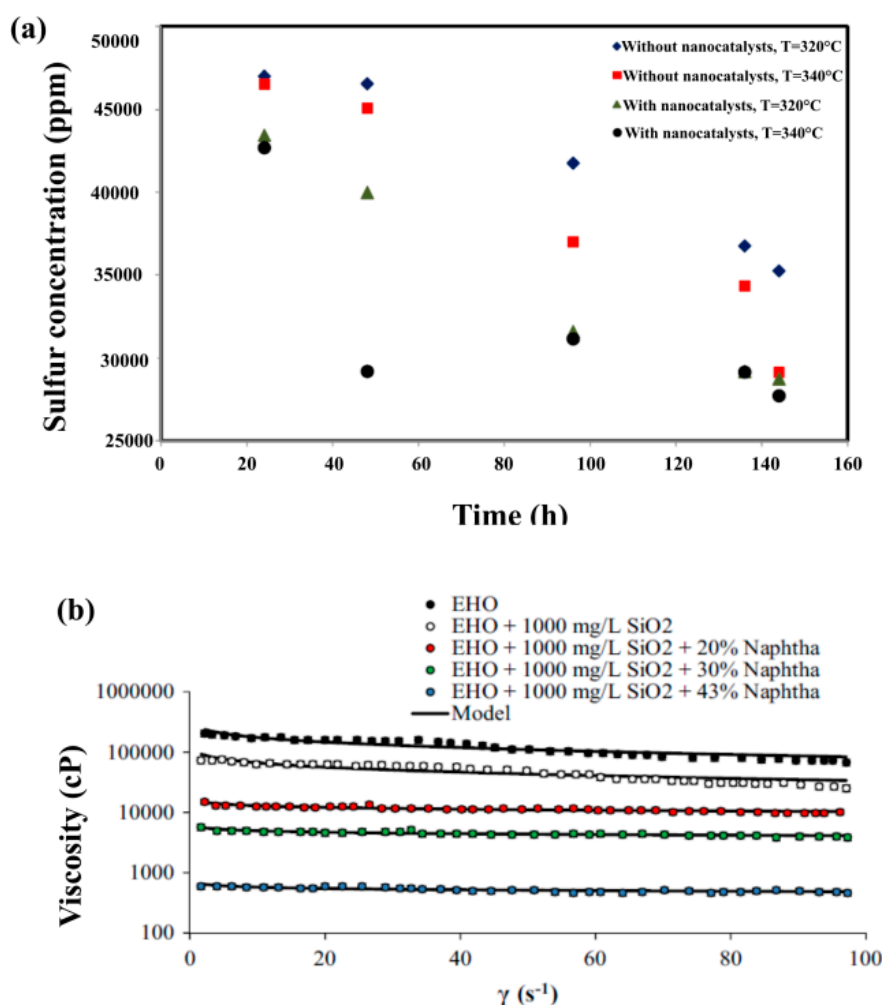


Figure 19. Positive environmental impacts. (a) Sulfur content of produced liquid samples from porous media at different times in the absence and presence of tri-metallic ultra-dispersed (UD) nanocatalysts. Reprinted with permission [157]; Copyright 2013, ACS Publications. (b) Viscosity and reduction consume of naphtha through the addition of 1000 mg·L⁻¹ of SiO₂. Reprinted with permission [92]; Copyright 2017, Elsevier.

10. Emerging Trends

Chemically based gas and water shut-off strategies by injection of gels or foams/emulsion and emulsion generation in presence of nanoparticles is a novel and recent strategy specifically aim to improve the mobility ratio between the injected EOR fluid and the reservoir crude oil. The existence of natural heterogeneities, such as zones of high permeability and fractures cause a decreasing in the sweep efficiency of the injected gas, in this sense the generation of emulsions and/or foams/emulsions or gels injection, are used as an alternative to block preferential channels. Thus, the injected fluid flows in the more permeable paths and it is forced to flow through the upswept regions. This behavior leads to higher oil displacement and an increase in sweep improving oil recovery.

Liquid foams are dispersions of gas bubbles in a continuous liquid phase, and are metastable systems [169]. Their unstable nature is a critical issue in a variety of well-established industrial applications. Most of the time, foams are stabilized using surface active agents such as surfactants adsorbed at the bubble surface. However, harsh reservoir conditions, high temperature, pressure, salinity, rock surface adsorption, and presence of electrolytes and solid particulate material in the lamellae decrease the stability of the foams and often limit their application in gas injection processes [170–175]. Recent studies show that NPs are able to improve the foam stability at severe reservoir conditions and subsequently oil recovery is improved. Inorganic oxide nanoparticles such as silica [176–182], Al_2O_3 [183–185], carbonate [186], TiO_2 [182], CuO [182], and fly ash nanoparticles [187,188] have been evaluated in foam stabilization. In particular, Figure 20a shows the oil recovery through waterflooding before (Step 1) and after (Step 2) the injection of surfactant (PSCI) in the absence (PSC1) and presence (PSC1 + SiO_2) of SiO_2 nanoparticles [177]. On another hand, in recent years nanoparticle-stabilized emulsions without surfactants or colloidal particles have gained great interest. SiO_2 [189,190], hydrophilic/hydrophobic silica [191,192], silica nanospheres [190], $\gamma\text{-Al}_2\text{O}_3$ [193] nanoparticles have evidenced O/W emulsions stabilized emulsion.

Another interesting water shut-off strategy to improve the volumetric sweep efficiency is related to the injection of gels. Gels are mainly synthesized by the bond of a high molecular weight polymer with a crosslinker in the presence of additives. Partially hydrolyzed polyacrylamides (HPAM) [194–196] and xanthan gum [196,197] are the polymer commonly used in water shutoff applications due to low cost, high viscosity at low concentrations, and availability. In general, the gels have limitations such as degradation by the effect of harsh reservoir as well as the adsorption of the chemicals over the rock [198]. Recent works have reported that the inclusion of nanoparticles to gels improve its stability and viscoelastic properties stability under static and dynamic conditions [199,200]. In addition, higher oil recovery values are observed in the presence of nanoparticles as shown in Figure 20b [199]. Displacement tests showed that inclusion of Al_2O_3 nanoparticles to partially hydrolyzed polyacrylamide/resorcinol/formaldehyde gel systems increases 64% of oil recovery in comparison with the system in the absence of nanoparticles [199]. Furthermore, the enhancement of the thermal stability and viscoelastic properties by effect of the addition of zirconium (IV) hydroxide ($\text{Zr}(\text{OH})_4$) nanoparticles to organically crosslinked polyacrylamide (PAM) hydrogels using hydroquinone (HQ) and hexamethylenetetramine (HMT) have been reported [200]. To the best of our knowledge, there are just two studies in the specialized literature reporting on improvement of stability of gels in the presence of NPs. In this order of ideas, exhaustive investigations on improvement of stability of gel by effect of NPs must be carried out

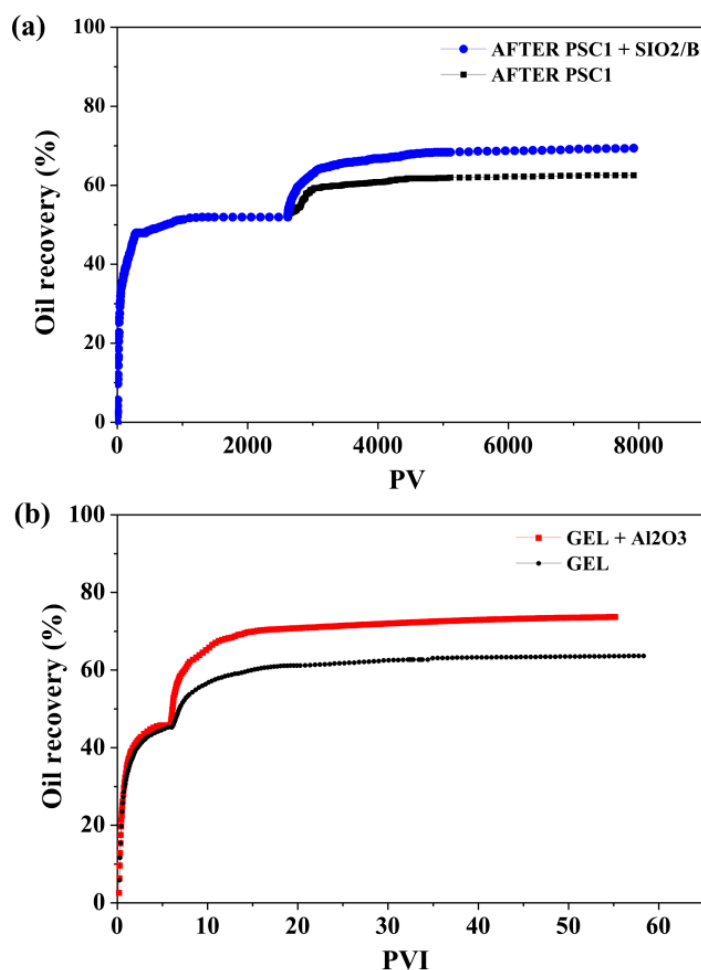


Figure 20. Oil recovery tests applying nanoparticles in foams and gels. (a) Oil recovery through waterflooding before (Step 1) and after (Step 2) the injection of surfactant (PSC1) in the absence (PSC1) and presence (PSC1 + SiO₂) of SiO₂ nanoparticles. Reprinted with permission [176]; Copyright 2018, ACS publications. (b) Oil recovery through waterflooding before (Step 1) and after (Step 2) the injection of gel in the absence (GEL) and presence (GEL + Al₂O₃) of Al₂O₃ nanoparticles. Reprinted with permission [199]; Copyright 2018, Wiley Periodicals, Inc.

11. Conclusions

In recent years, the application of nanoparticles in thermal oil recovery processes has attracted strong research interest. The current review shows that nanoparticles as adsorbent and catalysts have great potential applications for extra-heavy and heavy crude oil upgrading and recovery enhancement. Nanoparticles can decompose asphaltenes under different atmospheres, such as air, steam, inert, and even in electromagnetic treatments. This means that nanotechnology can effectively improve the efficiency of all thermal recovery processes (ISC, CSS, SAGD, THAI, THAI/Capri, among others). This is mainly due to the adsorptive and catalytic properties that the nanoparticles have, their high affinity for asphaltenes, and their capacity to accelerate the reactions that occurred under oxidative, gasification, and pyrolysis conditions.

In addition, thermal oil recovery by the addition of nanoparticles presents several advantages in terms of environmental and costs impacts: decreasing heat consumption, sulfur removal, reduction of water consumption, reduction of toxic chemical and capital costs, reduction of greenhouse gases, environmental remediation, and reduction of technology costs. Even though the application of nanoparticles in thermal oil recovery processes presents several advantages, exhaustive investigations on improving synthesis method of nanomaterials and expansion of applications of

existing nanomaterials need to be carried out. Finally, successful implementation of NPs to thermal oil recovery processes will facilitate the application of nanomaterials in the oil and gas industry.

Author Contributions: Conceptualization, O.M.E., C.O., F.B.C., and C.A.F.; investigation, O.E.M., C.O.; writing—original draft preparation, O.E.M. and C.O.; writing—review and editing, all authors.

Funding: The authors would like to acknowledge to FONDO NACIONAL DE FINANCIAMIENTO PARA LA CIENCIA, LA TECNOLOGÍA Y LA INNOVACIÓN “FRANCISCO JOSÉ DE CALDAS”, AGENCIA NACIONAL DE HIDROCARBUROS and COLCIENCIAS for their support provided in Agreement 272 of 2017. We would also like to recognize the Universidad Nacional de Colombia for logistical and financial support

Acknowledgments: The authors also acknowledge Grupo de Investigación en Fenómenos de Superficie—Michael Polanyi.

Conflicts of Interest: The authors declare no conflict of interest.

Nomenclature

CNC	Cellulose nanocrystals
CNS	Carbon nanospheres
CSS	Cyclic Steam Simulation
EHO	Extra-heavy crude oil
EM	Electromagnetic heating
EOR	Enhanced oil recovery
HMT	Hexamethylenetetramine
HO	Heavy crude oil
HPAM	Partially hydrolyzed polyacrylamides
HP-DSC	High-pressure differential scan
HQ	Hydroquinone
HTHP	High temperature and high pressure
IEA	International Energy Agency
IFT	Interfacial Tension
IOR	Improved Oil Recovery
ISC	In-Situ Combustion
NPs	Nanoparticles
PAM	Polyacrylamide
SAGD	Steam-Assisted Gravity Drainage
SBA-15	Mesoporous silica
SLE	Solid-Liquid Equilibrium
RF	Recovery factor
THAI	Toe-to-Heel Air Injection
THAI/CAPRI	Toe-to-Heel Air Injection (catalytic PRI)
TEO	Transition element oxides
TEOR	Thermal enhanced oil recovery
TGA	Thermal Gravimetric Analysis

References

1. Olsson, G. *Water and Energy: Threats and Opportunities*; IWA publishing: London, UK, 2015.
2. Shah, A.; Fishwick, R.; Wood, J.; Leeke, G.; Rigby, S.; Greaves, M. A review of novel techniques for heavy oil and bitumen extraction and upgrading. *Energy Environ. Sci.* **2010**, *3*, 700–714. [[CrossRef](#)]
3. International Energy Agency. *World Energy Outlook 2017*; International Energy Agency: Paris, France, 2017.
4. Tedeschi, M. RESERVES AND PRODUCTION OF HEAVY CRUDE OIL AND NATURAL BITUMEN. In Proceedings of the 13th World Petroleum Congress, Buenos Aires, Argentina, 1 January 1991; p. 8.
5. Miller, R.G.; Sorrell, S.R. *The Future of Oil Supply*; The Royal Society Publishing: London, UK, 2014.
6. Santos, R.; Loh, W.; Bannwart, A.; Trevisan, O. An overview of heavy oil properties and its recovery and transportation methods. *Braz. J. Chem. Eng.* **2014**, *31*, 571–590. [[CrossRef](#)]

7. Guo, K.; Li, H.; Yu, Z. In-situ heavy and extra-heavy oil recovery: A review. *Fuel* **2016**, *185*, 886–902. [[CrossRef](#)]
8. Guarín Arenas, F.; García, C.A.; Díaz Prada, C.A.; Cotes Leon, E.D.J.; Santos, N. A New Inflow Model for Extra-Heavy Crude Oils: Case Study Chichimene Field, Colombia. In Proceedings of the SPE Latin American and Caribbean Petroleum Engineering Conference, Lima, Peru, 1–3 December 2010.
9. Valbuena, O.H.; Bernal, M.E.; Ramon, J.C.; Xiuxia, T. First Extra-Heavy-Oil Development in Caguan-Putumayo Basin, Colombia, Capella Field. In Proceedings of the SPE Heavy and Extra Heavy Oil Conference: Latin America, Medellín, Colombia, 24–26 September 2014.
10. Lopez Uribe, J.E.; Chaustre Ruiz, A.J.; Ayala Marin, C.A. Producing Extra-Heavy Oil From Llanos Basin, Colombia, Through Progressive Cavity Pumps and Electric Submersible Pumps: Case Study in the Chichimene Field. In Proceedings of the SPE Heavy and Extra Heavy Oil Conference: Latin America, Medellín, Colombia, 24–26 September 2014.
11. Muggeridge, A.; Cockin, A.; Webb, K.; Frampton, H.; Collins, I.; Moulds, T.; Salino, P. Recovery rates, enhanced oil recovery and technological limits. *Philos. Trans. R. Soc. A Math. Phys. Eng. Sci.* **2014**, *372*, 20120320. [[CrossRef](#)]
12. Alvarado, V.; Manrique, E. Enhanced oil recovery: An update review. *Energies* **2010**, *3*, 1529–1575. [[CrossRef](#)]
13. Betancur, S.; Franco, C.A.; Cortés, F.B. Magnetite-silica nanoparticles with a core-shell structure for inhibiting the formation damage caused by the precipitation/deposition of asphaltene. *J. Magnetohydrodyn. Plasma Res.* **2016**, *21*, 289–322.
14. Betancur, S.; Giraldo, L.J.; Carrasco-Marín, F.; Riazi, M.; Manrique, E.J.; Quintero, H.; García, H.A.; Franco-Ariza, C.A.; Cortés, F.B. Importance of the Nanofluid Preparation for Ultra-Low Interfacial Tension in Enhanced Oil Recovery Based on Surfactant–Nanoparticle–Brine System Interaction. *ACS Omega* **2019**, *4*, 16171–16180. [[CrossRef](#)]
15. Yarveicy, H.; Habibi, A.; Pegov, S.; Zolfaghari, A.; Dehghanpour, H. Enhancing oil recovery by adding surfactants in fracturing water: A Montney case study. In Proceedings of the SPE Canada Unconventional Resources Conference, Calgary, AB, Canada, 13–14 March 2018.
16. Sheng, J. *Modern Chemical Enhanced Oil Recovery: Theory and Practice*; Gulf Professional Publishing: Oxford, UK, 2010.
17. Assef, Y.; Pereira Almaso, P. Evaluation of Cyclic Gas Injection in Enhanced Recovery from Unconventional Light Oil Reservoirs: Effect of Gas Type and Fracture Spacing. *Energies* **2019**, *12*, 1370. [[CrossRef](#)]
18. Alagorni, A.H.; Yaacob, Z.B.; Nour, A.H. An overview of oil production stages: Enhanced oil recovery techniques and nitrogen injection. *Int. J. Environ. Sci. Dev.* **2015**, *6*, 693. [[CrossRef](#)]
19. Caudle, B.; Dyes, A. Improving Miscible Displacement by Gas-Water Injection. In Proceedings of the 32nd Annual Fall Meeting of Society of Petroleum Engineers, Dallas, TX, USA, 6–9 October 1957.
20. Jia, B.; Tsau, J.-S.; Barati, R. A review of the current progress of CO₂ injection EOR and carbon storage in shale oil reservoirs. *Fuel* **2019**, *236*, 404–427. [[CrossRef](#)]
21. Zhang, Y.; Huang, S.S.; Luo, P. Coupling immiscible CO₂ technology and polymer injection to maximize EOR performance for heavy oils. *J. Can. Pet. Technol.* **2010**, *49*, 25–33. [[CrossRef](#)]
22. Song, C. Global challenges and strategies for control, conversion and utilization of CO₂ for sustainable development involving energy, catalysis, adsorption and chemical processing. *Catal. Today* **2006**, *115*, 2–32. [[CrossRef](#)]
23. Sun, X.; Zhang, Y.; Chen, G.; Gai, Z. Application of nanoparticles in enhanced oil recovery: A critical review of recent progress. *Energies* **2017**, *10*, 345. [[CrossRef](#)]
24. Yi, S.; Babadagli, T.; Li, H.A. Use of nickel nanoparticles for promoting aquathermolysis reaction during cyclic steam stimulation. *SPE J.* **2018**, *23*, 145–156. [[CrossRef](#)]
25. Jorshari, K.; O'Hara, B. A new SAGD-well-pair placement: A field case review. *J. Can. Pet. Technol.* **2013**, *52*, 12–19. [[CrossRef](#)]
26. Kar, T.; Ovalles, C.; Rogel, E.; Vien, J.; Hascakir, B. The residual oil saturation determination for Steam Assisted Gravity Drainage (SAGD) and Solvent-SAGD. *Fuel* **2016**, *172*, 187–195. [[CrossRef](#)]
27. Burger, J.G. Chemical aspects of in-situ combustion-heat of combustion and kinetics. *Soc. Pet. Eng. J.* **1972**, *12*, 410–422. [[CrossRef](#)]
28. Medina, O.E.; Gallego, J.; Rodríguez, E.; Franco, C.A.; Cortés, F.B. Effect of Pressure on the Oxidation Kinetics of Asphaltenes. *Energy Fuels* **2019**, *33*, 10734–10744. [[CrossRef](#)]

29. Franco, C.A.; Zabala, R.; Cortés, F.B. Nanotechnology applied to the enhancement of oil and gas productivity and recovery of Colombian fields. *J. Pet. Sci. Eng.* **2017**, *157*, 39–55. [[CrossRef](#)]
30. Franco, C.; Cardona, L.; Lopera, S.; Mejía, J.; Cortés, F. Heavy oil upgrading and enhanced recovery in a continuous steam injection process assisted by nanoparticulated catalysts. In Proceedings of the SPE improved oil recovery conference, Tulsa, OK, USA, 11–13 April 2016.
31. Iskandar, F.; Dwinanto, E.; Abdullah, M.; Muraza, O. Viscosity reduction of heavy oil using nanocatalyst in aquathermolysis reaction. *KONA Powder Part. J.* **2016**, *33*, 3–16. [[CrossRef](#)]
32. Hashemi, R.; Nassar, N.N.; Pereira Almaso, P. Enhanced heavy oil recovery by in situ prepared ultradispersed multimetallic nanoparticles: A study of hot fluid flooding for Athabasca bitumen recovery. *Energy Fuels* **2013**, *27*, 2194–2201. [[CrossRef](#)]
33. Montoya, T.; Argel, B.L.; Nassar, N.N.; Franco, C.A.; Cortés, F.B. Kinetics and mechanisms of the catalytic thermal cracking of asphaltenes adsorbed on supported nanoparticles. *Pet. Sci.* **2016**, *13*, 561–571. [[CrossRef](#)]
34. Husein, M.M.; Alkhaldi, S.J. In Situ Preparation of Alumina Nanoparticles in Heavy Oil and Their Thermal Cracking Performance. *Energy Fuels* **2014**, *28*, 6563–6569. [[CrossRef](#)]
35. Hou, J.; Li, C.; Gao, H.; Chen, M.; Huang, W.; Chen, Y.; Zhou, C. Recyclable oleic acid modified magnetic NiFe₂O₄ nanoparticles for catalytic aquathermolysis of Liaohe heavy oil. *Fuel* **2017**, *200*, 193–198. [[CrossRef](#)]
36. Kaminski, T.; Anis, S.F.; Husein, M.M.; Hashaiekh, R. Hydrocracking of Athabasca VR Using NiO-WO₃ Zeolite-Based Catalysts. *Energy Fuels* **2018**, *32*, 2224–2233. [[CrossRef](#)]
37. Franco, C.A.; Nassar, N.N.; Montoya, T.; Ruiz, M.A.; Cortés, F.B. Influence of Asphaltene Aggregation on the Adsorption and Catalytic Behavior of Nanoparticles. *Energy Fuels* **2015**, *29*, 1610–1621. [[CrossRef](#)]
38. Amrollahi Biyouki, A.; Hosseinpour, N.; Nassar, N.N. Pyrolysis and Oxidation of Asphaltene-Born Coke-like Residue Formed onto in Situ Prepared NiO Nanoparticles toward Advanced in Situ Combustion Enhanced Oil Recovery Processes. *Energy Fuels* **2018**, *32*, 5033–5044. [[CrossRef](#)]
39. Tang, X.-D.; Liang, G.-J.; Li, J.-J.; Wei, Y.-T.; Dang, T. Catalytic effect of in-situ preparation of copper oxide nanoparticles on the heavy oil low-temperature oxidation process in air injection recovery. *Pet. Sci. Technol.* **2017**, *35*, 1321–1326. [[CrossRef](#)]
40. Franco-Ariza, C.A.; Guzmán-Calle, J.D.; Cortés-Correa, F.B. Adsorption and catalytic oxidation of asphaltenes in fumed silica nanoparticles: Effect of the surface acidity. *Dyna* **2016**, *83*, 171–179. [[CrossRef](#)]
41. Nassar, N.N.; Hassan, A.; Pereira-Almaso, P. Comparative oxidation of adsorbed asphaltenes onto transition metal oxide nanoparticles. *Colloids Surf. A Physicochem. Eng. Asp.* **2011**, *384*, 145–149. [[CrossRef](#)]
42. Hosseinpour, N.; Mortazavi, Y.; Bahramian, A.; Khodatars, L.; Khodadadi, A.A. Enhanced pyrolysis and oxidation of asphaltenes adsorbed onto transition metal oxides nanoparticles towards advanced in-situ combustion EOR processes by nanotechnology. *Appl. Catal. A Gen.* **2014**, *477*, 159–171. [[CrossRef](#)]
43. Amrollahi Biyouki, A.; Hosseinpour, N.; Bahramian, A.; Vatani, A. In-situ upgrading of reservoir oils by in-situ preparation of NiO nanoparticles in thermal enhanced oil recovery processes. *Colloids Surf. A Physicochem. Eng. Asp.* **2017**, *520*, 289–300. [[CrossRef](#)]
44. Nassar, N.N.; Hassan, A.; Pereira-Almaso, P. Thermogravimetric studies on catalytic effect of metal oxide nanoparticles on asphaltene pyrolysis under inert conditions. *J. Therm. Anal. Calorim.* **2012**, *110*, 1327–1332. [[CrossRef](#)]
45. Nassar, N.N.; Franco, C.A.; Montoya, T.; Cortés, F.B.; Hassan, A. Effect of oxide support on Ni–Pd bimetallic nanocatalysts for steam gasification of n-C₇ asphaltenes. *Fuel* **2015**, *156*, 110–120. [[CrossRef](#)]
46. López, D.; Giraldo, L.J.; Salazar, J.P.; Zapata, D.M.; Ortega, D.C.; Franco, C.A.; Cortés, F.B. Metal Oxide Nanoparticles Supported on Macro-Mesoporous Aluminosilicates for Catalytic Steam Gasification of Heavy Oil Fractions for On-Site Upgrading. *Catalysts* **2017**, *7*, 319. [[CrossRef](#)]
47. Vélez, J.F.; Chejne, F.; Valdés, C.F.; Emery, E.J.; Londoño, C.A. Co-gasification of Colombian coal and biomass in fluidized bed: An experimental study. *Fuel* **2009**, *88*, 424–430. [[CrossRef](#)]
48. Nassar, N.N.; Hassan, A.; Luna, G.; Pereira-Almaso, P. Kinetics of the catalytic thermo-oxidation of asphaltenes at isothermal conditions on different metal oxide nanoparticle surfaces. *Catal. Today* **2013**, *207*, 127–132. [[CrossRef](#)]
49. Cardona, L.; Arias-Madrid, D.; Cortés, F.B.; Lopera, S.H.; Franco, C.A. Heavy Oil Upgrading and Enhanced Recovery in a Steam Injection Process Assisted by NiO-and PdO-Functionalized SiO₂ Nanoparticulated Catalysts. *Catalysts* **2018**, *8*, 132. [[CrossRef](#)]

50. Hashemi, R.; Nassar, N.N.; Almao, P.P. Nanoparticle technology for heavy oil in-situ upgrading and recovery enhancement: Opportunities and challenges. *Appl. Energy* **2014**, *133*, 374–387. [\[CrossRef\]](#)
51. Medina, O.E.; Gallego, J.; Restrepo, L.G.; Cortés, F.B.; Franco, C.A. Influence of the Ce⁴⁺/Ce³⁺ Redox-Couple on the Cyclic Regeneration for Adsorptive and Catalytic Performance of NiO-PdO/CeO₂±δ Nanoparticles for n-C7 Asphaltene Steam Gasification. *Nanomaterials* **2019**, *9*, 734. [\[CrossRef\]](#)
52. Ehtesabi, H.; Ahadian, M.M.; Taghikhani, V. Enhanced Heavy Oil Recovery Using TiO₂ Nanoparticles: Investigation of Deposition during Transport in Core Plug. *Energy Fuels* **2015**, *29*, 1–8. [\[CrossRef\]](#)
53. Amanam, U.U.; Kovscek, A.R. Analysis of the effects of copper nanoparticles on in-situ combustion of extra heavy-crude oil. *J. Pet. Sci. Eng.* **2017**, *152*, 406–415. [\[CrossRef\]](#)
54. Guo, K.; Li, H.; Yu, Z. Metallic Nanoparticles for Enhanced Heavy Oil Recovery: Promises and Challenges. *Energy Procedia* **2015**, *75*, 2068–2073. [\[CrossRef\]](#)
55. Heim, W.; Wolf, F.J.; Savery, W.T. Heavy Oil Recovering. Google Patents No. 4,456,065, 26 June 1984.
56. Yaws, C.L. *Yaws Handbook of Physical Properties for Hydrocarbons and Chemicals*; Elsevier: Amsterdam, The Netherlands, 2015.
57. Dianatnasab, F.; Nikookar, M.; Hosseini, S.; Sabeti, M. Study of reservoir properties and operational parameters influencing in the steam assisted gravity drainage process in heavy oil reservoirs by numerical simulation. *Petroleum* **2016**, *2*, 236–251. [\[CrossRef\]](#)
58. McCain, W.D., Jr. *Properties of Petroleum Fluids*; PennWell Corporation: Tulsa, OK, USA, 2017.
59. Rudyk, S. Relationships between SARA fractions of conventional oil, heavy oil, natural bitumen and residues. *Fuel* **2018**, *216*, 330–340. [\[CrossRef\]](#)
60. Liu, D.; Song, Q.; Tang, J.; Zheng, R.; Yao, Q. Interaction between saturates, aromatics and resins during pyrolysis and oxidation of heavy oil. *J. Pet. Sci. Eng.* **2017**, *154*, 543–550. [\[CrossRef\]](#)
61. Aske, N.; Kallevik, H.; Sjöblom, J. Determination of saturate, aromatic, resin, and asphaltenic (SARA) components in crude oils by means of infrared and near-infrared spectroscopy. *Energy Fuels* **2001**, *15*, 1304–1312. [\[CrossRef\]](#)
62. Vitolo, S.; Seggiani, M.; Filippi, S.; Brocchini, C. Recovery of vanadium from heavy oil and Orimulsion fly ashes. *Hydrometallurgy* **2000**, *57*, 141–149. [\[CrossRef\]](#)
63. Hossain, M.S.; Sarica, C.; Zhang, H.-Q.; Rhyne, L.; Greenhill, K. Assessment and development of heavy oil viscosity correlations. In Proceedings of the SPE International Thermal Operations and Heavy Oil Symposium, Calgary, AB, Canada, 1–3 November 2005.
64. Spiecker, P.M.; Gawrys, K.L.; Kilpatrick, P.K. Aggregation and solubility behavior of asphaltenes and their subfractions. *J. Colloid Interface Sci.* **2003**, *267*, 178–193. [\[CrossRef\]](#)
65. Mullins, O.C.; Sheu, E.Y.; Hammami, A.; Marshall, A.G. *Asphaltenes, Heavy Oils, and Petroleomics*; Springer Science & Business Media: New York, NY, USA, 2007.
66. Murgich, J. Intermolecular forces in aggregates of asphaltenes and resins. *Pet. Sci. Technol.* **2002**, *20*, 983–997. [\[CrossRef\]](#)
67. Mullins, O.C.; Sabbah, H.; Eyssautier, J.; Pomerantz, A.E.; Barré, L.; Andrews, A.B.; Ruiz-Morales, Y.; Mostowfi, F.; McFarlane, R.; Goual, L. Advances in asphaltene science and the Yen–Mullins model. *Energy Fuels* **2012**, *26*, 3986–4003. [\[CrossRef\]](#)
68. Mullins, O.C.; Pomerantz, A.E.; Andrews, A.B.; Majumdar, R.D.; Hazendonk, P.; Ruiz-Morales, Y.; Goual, L.; Zare, R.N. *Asphaltenes*. In *Springer Handbook of Petroleum Technology*; Springer: Cham, Switzerland, 2017; pp. 221–250.
69. Acevedo, S.; Castro, A.; Negrin, J.G.; Fernández, A.; Escobar, G.; Piscitelli, V.; Delolme, F.; Dessalces, G. Relations between asphaltene structures and their physical and chemical properties: The rosary-type structure. *Energy Fuels* **2007**, *21*, 2165–2175. [\[CrossRef\]](#)
70. Acevedo, S.; Castillo, J.; Vargas, V.; Castro, A.; Delgado, O.Z.; Ariza, C.A.F.; Cotés, F.B.; Bouyssiere, B. Suppression of Phase Separation as a Hypothesis to Account for Nuclei or Nanoaggregate Formation by Asphaltenes in Toluene. *Energy Fuels* **2018**, *32*, 6669–6677. [\[CrossRef\]](#)
71. Acevedo, S.; Castro, A.; Vásquez, E.; Marcano, F.; Ranaudo, M.A. Investigation of physical chemistry properties of asphaltenes using solubility parameters of asphaltenes and their fractions A1 and A2. *Energy Fuels* **2010**, *24*, 5921–5933. [\[CrossRef\]](#)

72. León, O.; Contreras, E.; Rogel, E.; Dambakli, G.; Acevedo, S.; Carbognani, L.; Espidel, J. Adsorption of native resins on asphaltene particles: A correlation between adsorption and activity. *Langmuir* **2002**, *18*, 5106–5112. [\[CrossRef\]](#)
73. Lozano, M.M.; Franco, C.A.; Acevedo, S.A.; Nassar, N.N.; Cortés, F.B. Effects of resin I on the catalytic oxidation of n-C 7 asphaltenes in the presence of silica-based nanoparticles. *RSC Adv.* **2016**, *6*, 74630–74642. [\[CrossRef\]](#)
74. Pérez, N.A.; Rincón, G.; Velásquez, J. Effect of resin and asphaltene content present on the vacuum residue on the yield of delayed coking products (Efecto del contenido de resinas y asfaltenos presente en el residuo de vacío sobre el rendimiento de los productos de la coquización retardada). *Rev. Latinoam. de Metal. y Mater.* **2019**, *39*, 1–10.
75. Pereira, J.; López, I. Interacciones resinas-asfaltenos: Correlación con la precipitación de asfaltenos. *Ciencia* **2006**, *14*, 132–142.
76. Navarro, L.; Álvarez, M.; Grosso, J.-L.; Navarro, U. Separación y caracterización de resinas y asfaltenos provenientes del crudo Castilla. Evaluación de su interacción molecular. *CT&F-Ciencia, Tecnología y Futuro* **2004**, *2*, 53–67.
77. Andersen, S.I.; Speight, J.G. Petroleum resins: Separation, character, and role in petroleum. *Pet. Sci. Technol.* **2001**, *19*, 1–34. [\[CrossRef\]](#)
78. Behura, J.; Batzle, M.; Hofmann, R.; Dorgan, J. Heavy oils: Their shear story. *Geophysics* **2007**, *72*, E175–E183. [\[CrossRef\]](#)
79. Wang, J.; Anthony, E.J. A study of thermal-cracking behavior of asphaltenes. *Chem. Eng. Sci.* **2003**, *58*, 157–162. [\[CrossRef\]](#)
80. Inoue, S.-I.; Takatsuka, T.; Wada, Y.; Nakata, S.-I.; Ono, T. A new concept for catalysts of asphaltene conversion. *Catal. Today* **1998**, *43*, 225–232. [\[CrossRef\]](#)
81. Liao, Z.; Geng, A. Characterization of nC7-soluble fractions of the products from mild oxidation of asphaltenes. *Org. Geochem.* **2002**, *33*, 1477–1486. [\[CrossRef\]](#)
82. Franco, C.A.; Montoya, T.; Nassar, N.N.; Pereira-Almao, P.; Cortés, F.B. Adsorption and subsequent oxidation of colombian asphaltenes onto nickel and/or palladium oxide supported on fumed silica nanoparticles. *Energy Fuels* **2013**, *27*, 7336–7347. [\[CrossRef\]](#)
83. Stell, R.C.; Dinicolantonio, A.R.; Frye, J.M.; Spicer, D.B.; McCoy, J.N.; Strack, R.D. Process for Steam Cracking Heavy Hydrocarbon Feedstocks. Google Patents Application No. 7,138,047, 21 November 2006.
84. Franco, C.A.; Montoya, T.; Nassar, N.N.; Cortés, F.B. NiO and PdO Supported on Fumed Silica Nanoparticles for Adsorption and Catalytic Steam Gasification of Colombian n-C7 Asphaltenes. In *Handbook on Oil Production Research*; Nova Science Publishers: Hauppauge, NY, USA, 2014; pp. 101–145.
85. Gray, M.R. Consistency of asphaltene chemical structures with pyrolysis and coking behavior. *Energy Fuels* **2003**, *17*, 1566–1569. [\[CrossRef\]](#)
86. Ambalae, A.; Mahinpey, N.; Freitag, N. Thermogravimetric studies on pyrolysis and combustion behavior of a heavy oil and its asphaltenes. *Energy Fuels* **2006**, *20*, 560–565. [\[CrossRef\]](#)
87. Cardona Rojas, L. Efecto de nanopartículas en procesos con inyección de vapor a diferentes calidades. Master's Thesis, Universidad Nacional de Colombia-Sede Medellín, Medellín, Colombia, 2018.
88. Medina, O.E.; Gallego, J.; Arias-Madrid, D.; Cortés, F.B.; Franco, C.A. Optimization of the Load of Transition Metal Oxides (Fe₂O₃, Co₃O₄, NiO and/or PdO) onto CeO₂ Nanoparticles in Catalytic Steam Decomposition of n-C7 Asphaltenes at Low Temperatures. *Nanomaterials* **2019**, *9*, 401. [\[CrossRef\]](#)
89. Niu, B.; Ren, S.; Liu, Y.; Wang, D.; Tang, L.; Chen, B. Low-temperature oxidation of oil components in an air injection process for improved oil recovery. *Energy Fuels* **2011**, *25*, 4299–4304. [\[CrossRef\]](#)
90. Adams, J.J. Asphaltene adsorption, a literature review. *Energy Fuels* **2014**, *28*, 2831–2856. [\[CrossRef\]](#)
91. Cortés, F.B.; Montoya, T.; Acevedo, S.; Nassar, N.N.; Franco, C.A. Adsorption-desorption of n-c7 asphaltenes over micro-and nanoparticles of silica and its impact on wettability alteration. *CT F-Ciencia, Tecnología y Futuro* **2016**, *6*, 89–106. [\[CrossRef\]](#)
92. Taborda, E.A.; Alvarado, V.; Cortés, F.B. Effect of SiO₂-based nanofluids in the reduction of naphtha consumption for heavy and extra-heavy oils transport: Economic impacts on the Colombian market. *Energy Convers. Manag.* **2017**, *148*, 30–42. [\[CrossRef\]](#)

93. Taborda, E.A.; Franco, C.A.; Lopera, S.H.; Alvarado, V.; Cortés, F.B. Effect of nanoparticles/nanofluids on the rheology of heavy crude oil and its mobility on porous media at reservoir conditions. *Fuel* **2016**, *184*, 222–232. [[CrossRef](#)]
94. Taborda, E.A.; Alvarado, V.; Franco, C.A.; Cortés, F.B. Rheological demonstration of alteration in the heavy crude oil fluid structure upon addition of nanoparticles. *Fuel* **2017**, *189*, 322–333. [[CrossRef](#)]
95. Acevedo, S.C.; García, L.A.; Rodríguez, P. Changes of diameter distribution with temperature measured for asphaltenes and their fractions A1 and A2. Impact of these measurements in colloidal and solubility issues of asphaltenes. *Energy Fuels* **2012**, *26*, 1814–1819. [[CrossRef](#)]
96. Nassar, N.N. Asphaltene adsorption onto alumina nanoparticles: Kinetics and thermodynamic studies. *Energy Fuels* **2010**, *24*, 4116–4122. [[CrossRef](#)]
97. Márquez, S.B.; Cortés, F.B.; Marín, F.C. Desarrollo de Nanopartículas Basadas en Sílice para la Inhibición de la Precipitación/Deposición de Asfaltenos. In *Química y Petróleos*; Universidad Nacional de Colombia: Medellín, Colombia, 2015; p. 96.
98. Nassar, N.N.; Montoya, T.; Franco, C.A.; Cortés, F.B.; Pereira-Almao, P. A new model for describing the adsorption of asphaltenes on porous media at a high pressure and temperature under flow conditions. *Energy Fuels* **2015**, *29*, 4210–4221. [[CrossRef](#)]
99. Cortés, F.B.; Mejía, J.M.; Ruiz, M.A.; Benjumea, P.; Riffel, D.B. Sorption of asphaltenes onto nanoparticles of nickel oxide supported on nanoparticulated silica gel. *Energy Fuels* **2012**, *26*, 1725–1730. [[CrossRef](#)]
100. Franco, C.A.; Lozano, M.M.; Acevedo, S.; Nassar, N.N.; Cortés, F.B. Effects of resin I on asphaltene adsorption onto nanoparticles: A novel method for obtaining asphaltenes/resin isotherms. *Energy Fuels* **2015**, *30*, 264–272. [[CrossRef](#)]
101. Nassar, N.N.; Hassan, A.; Pereira-Almao, P. Effect of surface acidity and basicity of aluminas on asphaltene adsorption and oxidation. *J. Colloid Interface Sci.* **2011**, *360*, 233–238. [[CrossRef](#)]
102. Shayan, N.N.; Mirzayi, B. Adsorption and removal of asphaltene using synthesized maghemite and hematite nanoparticles. *Energy Fuels* **2015**, *29*, 1397–1406. [[CrossRef](#)]
103. Marei, N.N.; Nassar, N.N.; Vitale, G. The effect of the nanosize on surface properties of NiO nanoparticles for the adsorption of Quinolin-65. *Phys. Chem. Chem. Phys.* **2016**, *18*, 6839–6849. [[CrossRef](#)] [[PubMed](#)]
104. Diez, R.; Giraldo, L.J.; Arias Madrid, D.; Gallego Marin, J.; Cortés, F.B.; Franco Ariza, C. Síntesis y caracterización de nanopartículas Janus de sílice/níquel para procesos EOR por inyección de vapor. In Proceedings of the Congreso Mexicano del Petróleo, Mexico city, Mexico, 26–29 September 2018.
105. Giraldo, L.J.; Gallego, J.; Villegas, J.P.; Franco, C.A.; Cortés, F.B. Enhanced waterflooding with NiO/SiO₂ 0-D Janus nanoparticles at low concentration. *J. Pet. Sci. Eng.* **2019**, *174*, 40–48. [[CrossRef](#)]
106. Franco, C.A.; Nassar, N.N.; Ruiz, M.A.; Pereira-Almao, P.; Cortés, F.B. Nanoparticles for inhibition of asphaltenes damage: Adsorption study and displacement test on porous media. *Energy Fuels* **2013**, *27*, 2899–2907. [[CrossRef](#)]
107. Nassar, N.N.; Hassan, A.; Pereira-Almao, P. Metal oxide nanoparticles for asphaltene adsorption and oxidation. *Energy Fuels* **2011**, *25*, 1017–1023. [[CrossRef](#)]
108. Polanyi, M. The potential theory of adsorption. *Science* **1963**, *141*, 1010–1013. [[CrossRef](#)]
109. Montoya, T.; Coral, D.; Franco, C.A.; Nassar, N.N.; Cortés, F.B. A novel solid–liquid equilibrium model for describing the adsorption of associating asphaltene molecules onto solid surfaces based on the “chemical theory”. *Energy Fuels* **2014**, *28*, 4963–4975. [[CrossRef](#)]
110. Aristizábal-Fontal, J.E.; Cortés, F.B.; Franco, C.A. Viscosity reduction of extra heavy crude oil by magnetite nanoparticle-based ferrofluids. *Adsorpt. Sci. Technol.* **2017**, *36*, 23–45. [[CrossRef](#)]
111. Hamed Shokrlu, Y.; Babadagli, T. Effects of nano-sized metals on viscosity reduction of heavy oil/bitumen during thermal applications. In Proceedings of the Canadian Unconventional Resources and International Petroleum Conference, Calgary, AB, Canada, 19–21 October 2010.
112. Taborda, E.A.; Franco, C.A.; Ruiz, M.A.; Alvarado, V.; Cortés, F.B. Experimental and Theoretical Study of Viscosity Reduction in Heavy Crude Oils by Addition of Nanoparticles. *Energy Fuels* **2017**, *31*, 1329–1338. [[CrossRef](#)]
113. Montes, D.; Orozco, W.; Taborda, E.A.; Franco, C.A.; Cortés, F.B. Development of Nanofluids for Perdurability in Viscosity Reduction of Extra-Heavy Oils. *Energies* **2019**, *12*, 1068. [[CrossRef](#)]
114. Zhao, R.; Chen, Y.; Huan, R.; Castanier, L.M.; Kovscek, A.R. An experimental investigation of the in-situ combustion behavior of Karamay crude oil. *J. Pet. Sci. Eng.* **2015**, *127*, 82–92. [[CrossRef](#)]

115. Ado, M.R.; Greaves, M.; Rigby, S.P. Dynamic Simulation of the THAI Heavy Oil Recovery Process. *Energy Fuels* **2017**, *31*, 1276–1284.
116. Xia, T.; Greaves, M.; Turta, A. Main Mechanism for Stability of THAI-“Toe-to-Heel Air Injection”. In Proceedings of the Canadian International Petroleum Conference, Calgary, AB, Canada, 10–12 June 2003.
117. Thomas, S. Enhanced oil recovery-an overview. *Oil Gas Sci. Technol. -Revue de l'IFP* **2008**, *63*, 9–19. [[CrossRef](#)]
118. Greaves, M.; Xia, T.X.; Ayasse, C. Underground upgrading of heavy oil using THAI-‘toe-to-heel air injection’. In Proceedings of the SPE International Thermal Operations and Heavy Oil Symposium, Calgary, AB, Canada, 1–3 November 2005.
119. Hart, A. Advanced Studies of Catalytic Upgrading of Heavy Oils. Ph.D. Thesis, University of Birmingham, Birmingham, UK, 2014.
120. Greaves, M.; Xia, T. CAPRI-Downhole catalytic process for upgrading heavy oil: Produced oil properties and composition. In Proceedings of the Canadian international petroleum conference, Calgary, AB, Canada, 12–14 June 2001.
121. Hart, A.; Wood, J. In Situ Catalytic Upgrading of Heavy Crude with CAPRI: Influence of Hydrogen on Catalyst Pore Plugging and Deactivation due to Coke. *Energies* **2018**, *11*, 636. [[CrossRef](#)]
122. Marei, N.N.; Nassar, N.N.; Vitale, G.; Hassan, A.; Zurita, M.J.P. Effects of the size of NiO nanoparticles on the catalytic oxidation of Quinolin-65 as an asphaltene model compound. *Fuel* **2017**, *207*, 423–437. [[CrossRef](#)]
123. Marei, N.N.; Nassar, N.N.; Hmoudah, M.; El-Qanni, A.; Vitale, G.; Hassan, A. Nanosize effects of NiO nanosorbents on adsorption and catalytic thermo-oxidative decomposition of vacuum residue asphaltenes. *Can. J. Chem. Eng.* **2017**, *95*, 1864–1874. [[CrossRef](#)]
124. Mirzayi, B.; Shayan, N.N. Adsorption kinetics and catalytic oxidation of asphaltene on synthesized maghemite nanoparticles. *J. Pet. Sci. Eng.* **2014**, *121*, 134–141. [[CrossRef](#)]
125. Yuan, C.; Varfolomeev, M.A.; Emelianov, D.A.; Suwaid, M.A.; Khachatryan, A.A.; Starshinova, V.L.; Vakhitov, I.R.; Al-Muntaser, A.A. Copper stearate as a catalyst for improving the oxidation performance of heavy oil in in-situ combustion process. *Appl. Catal. A Gen.* **2018**, *564*, 79–89. [[CrossRef](#)]
126. Druetta, P.; Raffa, P.; Picchioni, F. Plenty of Room at the Bottom: Nanotechnology as Solution to an Old Issue in Enhanced Oil Recovery. *Appl. Sci.* **2018**, *8*, 2596. [[CrossRef](#)]
127. Luft, H.; Pelensky, P.; George, G. Development and operation of a new insulated concentric coiled tubing string for continuous steam injection in heavy oil production. In Proceedings of the SPE International Heavy Oil Symposium, Calgary, AB, Canada, 19–21 June 1995.
128. Boberg, T.C. *Thermal Methods of Oil Recovery*; Wiley: Hoboken, NJ, USA, 1988.
129. Hassan, A.; Carbognani-Arambarri, L.; Nassar, N.N.; Vitale, G.; Bartolini, M.; Pereira-Almao, P. Catalytic Steam Gasification of Athabasca Visbroken Residue by NiO–Kaolin-Based Catalysts in a Fixed-Bed Reactor. *Energy Fuels* **2017**, *31*, 7396–7404. [[CrossRef](#)]
130. Hassan, A.; Lopez-Linares, F.; Nassar, N.N.; Carbognani-Arambarri, L.; Pereira-Almao, P. Development of a support for a NiO catalyst for selective adsorption and post-adsorption catalytic steam gasification of thermally converted asphaltenes. *Catal. Today* **2013**, *207*, 112–118. [[CrossRef](#)]
131. Nassar, N.N.; Hassan, A.; Pereira-Almao, P. Application of nanotechnology for heavy oil upgrading: Catalytic steam gasification/cracking of asphaltenes. *Energy Fuels* **2011**, *25*, 1566–1570. [[CrossRef](#)]
132. Hamed Shokrlu, Y.; Babadagli, T. In-situ upgrading of heavy oil/bitumen during steam injection by use of metal nanoparticles: A study on in-situ catalysis and catalyst transportation. *SPE Reser. Eval. Eng.* **2013**, *16*, 333–344. [[CrossRef](#)]
133. Jeong, G.; Kim, C.H.; Hur, Y.G.; Han, G.-H.; Lee, S.H.; Lee, K.-Y. Ni-Doped MoS₂ Nanoparticles Prepared via Core–Shell Nanoclusters and Catalytic Activity for Upgrading Heavy Oil. *Energy Fuels* **2018**, *32*, 9263–9270. [[CrossRef](#)]
134. Betancur, S.; Carrasco-Marín, F.; Pérez-Cadenas, A.F.; Franco, C.A.; Jiménez, J.; Manrique, E.J.; Quintero, H.; Cortés, F.B. Effect of Magnetic Iron Core–Carbon Shell Nanoparticles in Chemical Enhanced Oil Recovery for Ultralow Interfacial Tension Region. *Energy Fuels* **2019**, *33*, 4158–4168. [[CrossRef](#)]
135. Maity, S.; Ancheyta, J.; Soberanis, L.; Alonso, F.; Llanos, M. Alumina–titania binary mixed oxide used as support of catalysts for hydrotreating of Maya heavy crude. *Appl. Catal. A Gen.* **2003**, *244*, 141–153. [[CrossRef](#)]
136. Gao, Y.; Ghorbanian, B.; Gargari, H.N.; Gao, W. Steam reforming of gaseous by-products from bitumen oil using various supported Ni-based catalysts. *Pet. Sci. Technol.* **2018**, *36*, 34–39. [[CrossRef](#)]

137. Hashemi, R.; Nassar, N.N.; Pereira-Almao, P. Transport behavior of multimetallic ultradispersed nanoparticles in an oil-sands-packed bed column at a high temperature and pressure. *Energy Fuels* **2012**, *26*, 1645–1655. [[CrossRef](#)]
138. Farooqui, J.; Babadagli, T.; Li, H.A. Improvement of the recovery factor using nano-metal particles at the late stages of cyclic steam stimulation. In Proceedings of the SPE Canada Heavy Oil Technical Conference, Calgary, AB, Canada, 9–11 June 2015.
139. Shen, Y.; Yoshikawa, K. Recent progresses in catalytic tar elimination during biomass gasification or pyrolysis—A review. *Renew. Sustain. Energy Rev.* **2013**, *21*, 371–392. [[CrossRef](#)]
140. Kapadia, P.R.; Kallos, M.S.; Gates, I.D. A review of pyrolysis, aquathermolysis, and oxidation of Athabasca bitumen. *Fuel Proc. Technol.* **2015**, *131*, 270–289. [[CrossRef](#)]
141. Douda, J.; Llanos, M.E.; Alvarez, R.; Franco, C.L.; de la Fuente, J.A.M. Pyrolysis applied to the study of a Maya asphaltene. *J. Anal. Appl. Pyrolysis* **2004**, *71*, 601–612. [[CrossRef](#)]
142. Magaril, R.; Aksenova, É. Investigation of the mechanism of coke formation during thermal decomposition of asphaltenes. *Chem. Technol. Fuels Oils* **1970**, *6*, 509–512. [[CrossRef](#)]
143. Rezaei, M.; Schaffie, M.; Ranjbar, M. Thermocatalytic in situ combustion: Influence of nanoparticles on crude oil pyrolysis and oxidation. *Fuel* **2013**, *113*, 516–521. [[CrossRef](#)]
144. Chhetri, A.; Islam, M. A critical review of electromagnetic heating for enhanced oil recovery. *Pet. Sci. Technol.* **2008**, *26*, 1619–1631. [[CrossRef](#)]
145. Mohd Zaid, H.; Latiff, A.; Rasyada, N.; Yahya, N.; Soleimani, H.; Shafie, A. Application of Electromagnetic Waves and Dielectric Nanoparticles in Enhanced Oil Recovery. *J. Nano Res.* **2014**, *26*, 135–142. [[CrossRef](#)]
146. Al-Shehri, A.A.; Ellis, E.S.; Servin, J.M.F.; Kosynkin, D.V.; Kanj, M.Y.; Schmidt, H.K. Illuminating the reservoir: Magnetic nanomappers. In Proceedings of the SPE Middle East Oil and Gas Show and Conference, Manama, Bahrain, 10–13 March 2013.
147. Greff, J.; Babadagli, T. Catalytic effects of nano-size metal ions in breaking asphaltene molecules during thermal recovery of heavy-oil. In Proceedings of the SPE Annual Technical Conference and Exhibition, Denver, CO, USA, 30 October–2 November 2011.
148. Yahya, N.; Kashif, M.; Nasir, N.; Niaz Akhtar, M.; Yusof, N.M. Cobalt ferrite nanoparticles: An innovative approach for enhanced oil recovery application. *J. Nano Res.* **2012**, *17*, 115–126. [[CrossRef](#)]
149. Hascakir, B.; Akin, S. Effect of metallic additives on upgrading heavy oil with microwave heating. In Proceedings of the First World Heavy Oil Conference, Beijing, China, 15 January 2006.
150. Shokrlu, Y.H.; Babadagli, T. Transportation and interaction of nano and micro size metal particles injected to improve thermal recovery of heavy-oil. In Proceedings of the SPE Annual Technical Conference and Exhibition, Denver, CO, USA, 30 October–2 November 2011.
151. Bennetzen, M.V.; Mogensen, K. Novel applications of nanoparticles for future enhanced oil recovery. In Proceedings of the International petroleum technology conference, Kuala Lumpur, Malaysia, 10–12 December 2014.
152. Nassar, N.N.; Betancur, S.; Acevedo, S.; Franco, C.A.; Cortés, F.B. Development of a Population Balance Model to Describe the Influence of Shear and Nanoparticles on the Aggregation and Fragmentation of Asphaltene Aggregates. *Ind. Eng. Chem. Res.* **2015**, *54*, 8201–8211. [[CrossRef](#)]
153. Guzmán, J.D.; Betancur, S.; Carrasco-Marín, F.; Franco, C.A.; Nassar, N.N.; Cortés, F.B. Importance of the Adsorption Method Used for Obtaining the Nanoparticle Dosage for Asphaltene-Related Treatments. *Energy Fuels* **2016**, *30*, 2052–2059. [[CrossRef](#)]
154. Li, L.; Yuan, X.; Sun, J. Vital role of nanotechnology and nanomaterials in the field of oilfield chemistry Soc. *Pet. Eng.* **2013**, *1*, 85–91.
155. Loria, H.; Trujillo-Ferrer, G.; Sosa-Stull, C.; Pereira-Almao, P. Kinetic Modeling of Bitumen Hydroprocessing at In-Reservoir Conditions Employing Ultradispersed Catalysts. *Energy Fuels* **2011**, *25*, 1364–1372. [[CrossRef](#)]
156. Hashemi, R.; Nassar, N.N.; Pereira Almao, P. In Situ Upgrading of Athabasca Bitumen Using Multimetallic Ultradispersed Nanocatalysts in an Oil Sands Packed-Bed Column: Part 2. Solid Analysis and Gaseous Product Distribution. *Energy Fuels* **2014**, *28*, 1351–1361. [[CrossRef](#)]
157. Galarraga, C.E.; Pereira-Almao, P. Hydrocracking of Athabasca Bitumen Using Submicronic Multimetallic Catalysts at Near In-Reservoir Conditions. *Energy Fuels* **2010**, *24*, 2383–2389. [[CrossRef](#)]

158. Hashemi, R.; Nassar, N.N.; Pereira Almaso, P. In Situ Upgrading of Athabasca Bitumen Using Multimetallic Ultradispersed Nanocatalysts in an Oil Sands Packed-Bed Column: Part 1. Produced Liquid Quality Enhancement. *Energy Fuels* **2013**, *28*, 1338–1350. [\[CrossRef\]](#)
159. Tajmimi, M.; Ehsani, M.R. The Potential of ZnO Nanoparticles to Reduce Water Consuming in Iranian Heavy Oil Reservoir. *J. Water Environ. Nanotechnol.* **2016**, *1*, 84–90. [\[CrossRef\]](#)
160. Al-Maamari, R.S.H.; Buckley, J.S. Asphaltene Precipitation and Alteration of Wetting: The Potential for Wettability Changes During Oil Production. *SPE Reserv. Eval. Eng.* **2003**, *6*, 210–214. [\[CrossRef\]](#)
161. Gharfeh, S.; Yen, A.; Asomaning, S.; Blumer, D. Asphaltene Flocculation Onset Determinations for Heavy Crude Oil and Its Implications. *Pet. Sci. Technol.* **2004**, *22*, 1055–1072. [\[CrossRef\]](#)
162. Oskui, G.; Reza, P.; Jumaa, M.A.; Folad, E.G.; Rashed, A.; Patil, S. Systematic approach for prevention and remediation of asphaltene problems during CO₂/hydrocarbon injection project. In Proceedings of the Twenty-first International Offshore and Polar Engineering Conference, Maui, HI, USA, 19–24 June 2011.
163. Kojima, T.; Tahara, K. Refinement and transportation of petroleum with hydrogen from renewable energy. *Energy Convers. Manag.* **2001**, *42*, 1839–1851. [\[CrossRef\]](#)
164. Aminzadeh, B.; Chung, D.; Bryant, S.L.; Huh, C.; DiCarlo, D.A. CO₂ leakage prevention by introducing engineered nanoparticles to the in-situ brine. *Energy Procedia* **2013**, *37*, 5290–5297. [\[CrossRef\]](#)
165. Karn, B.; Kuiken, T.; Otto, M. Nanotechnology and in situ remediation: A review of the benefits and potential risks. *Environ. Health Perspect.* **2009**, *117*, 1813–1831. [\[CrossRef\]](#)
166. Yunus, I.S.; Harwin; Kurniawan, A.; Adityawarman, D.; Indarto, A. Nanotechnologies in water and air pollution treatment. *Environ. Technol. Rev.* **2012**, *1*, 136–148. [\[CrossRef\]](#)
167. Qu, X.; Alvarez, P.J.J.; Li, Q. Applications of nanotechnology in water and wastewater treatment. *Water Res.* **2013**, *47*, 3931–3946. [\[CrossRef\]](#) [\[PubMed\]](#)
168. Youssif, M.I.; El-Maghraby, R.M.; Saleh, S.M.; Elgibaly, A. Silica nanofluid flooding for enhanced oil recovery in sandstone rocks. *Egypt. J. Pet.* **2018**, *27*, 105–110. [\[CrossRef\]](#)
169. Weaire, D.; Phelan, R. The physics of foam. *J. Phys. Condens. Matter* **1996**, *8*, 9519. [\[CrossRef\]](#)
170. Al-Hashim, H.S.; Celik, M.S.; Oskay, M.M.; Al-Yousef, H.Y. Adsorption and precipitation behaviour of petroleum sulfonates from Saudi Arabian limestone. *J. Pet. Sci. Eng.* **1988**, *1*, 335–344. [\[CrossRef\]](#)
171. Figdore, P.E. Adsorption of surfactants on kaolinite: NaCl versus CaCl₂ salt effects. *J. Colloid Interface Sci.* **1982**, *87*, 500–517. [\[CrossRef\]](#)
172. Khatib, Z.I.; Hirasaki, G.J.; Falls, A.H. Effects of Capillary Pressure on Coalescence and Phase Mobilities in Foams Flowing Through Porous Media. *SPE Reserv. Eng.* **1988**, *3*, 919–926. [\[CrossRef\]](#)
173. Farzaneh, S.A.; Sohrabi, M. A Review of the Status of Foam Application in Enhanced Oil Recovery. In Proceedings of the EAGE Annual Conference & Exhibition incorporating SPE Europepec, London, UK, 10 June 2013; p. 15.
174. Friedmann, F.; Chen, W.H.; Gauglitz, P.A. Experimental and Simulation Study of High-Temperature Foam Displacement in Porous Media. *SPE Reserv. Eng.* **1991**, *6*, 37–45. [\[CrossRef\]](#)
175. Zhang, Y.; Zhang, L.; Chen, B.; Li, H.K.; Wang, Y.T.; Ren, S.R. Evaluation and experimental study on CO₂ foams at high pressure and temperature. *J. Chem. Eng. Chin. Univ.* **2014**, *28*, 535–541.
176. Hurtado, Y.; Beltrán, C.; Zabala, R.D.; Lopera, S.H.; Franco, C.A.; Nassar, N.N.; Cortés, F.B. Effects of Surface Acidity and Polarity of SiO₂ Nanoparticles on the Foam Stabilization Applied to Natural Gas Flooding in Tight Gas-Condensate Reservoirs. *Energy Fuels* **2018**, *32*, 5824–5833. [\[CrossRef\]](#)
177. Hunter, T.N.; Pugh, R.J.; Franks, G.V.; Jameson, G.J. The role of particles in stabilising foams and emulsions. *Adv. Colloid Interface Sci.* **2008**, *137*, 57–81. [\[CrossRef\]](#)
178. Binks, B.P.; Horozov, T.S. Aqueous Foams Stabilized Solely by Silica Nanoparticles. *Angew. Chem. Int. Ed.* **2005**, *44*, 3722–3725. [\[CrossRef\]](#) [\[PubMed\]](#)
179. Wang, J.; Xue, G.; Tian, B.; Li, S.; Chen, K.; Wang, D.; Sun, Y.; Xu, H.; Petkov, J.T.; Li, Z. Interaction between Surfactants and SiO₂ Nanoparticles in Multiphase Foam and Its Plugging Ability. *Energy Fuels* **2017**, *31*, 408–417. [\[CrossRef\]](#)
180. Yusuf, S.; Manan, M.; Jaafar, M. Aqueous foams stabilized by hydrophilic silica nanoparticles via in-situ physisorption of nonionic TX100 Surfactant. *Iran. J. Energy Environ.* **2013**, *4*, 8–16.
181. Zhu, Y.; Pei, X.; Jiang, J.; Cui, Z.; Binks, B.P. Responsive aqueous foams stabilized by silica nanoparticles hydrophobized in situ with a conventional surfactant. *Langmuir* **2015**, *31*, 12937–12943. [\[CrossRef\]](#)

182. Manan, M.; Farad, S.; Piroozian, A.; Esmail, M. Effects of nanoparticle types on carbon dioxide foam flooding in enhanced oil recovery. *Pet. Sci. Technol.* **2015**, *33*, 1286–1294. [\[CrossRef\]](#)
183. Yekeen, N.; Manan, M.A.; Idris, A.K.; Samin, A.M.; Risal, A.R. Experimental investigation of minimization in surfactant adsorption and improvement in surfactant-foam stability in presence of silicon dioxide and aluminum oxide nanoparticles. *J. Pet. Sci. Eng.* **2017**, *159*, 115–134. [\[CrossRef\]](#)
184. Yekeen, N.; Idris, A.K.; Manan, M.A.; Samin, A.M.; Risal, A.R.; Kun, T.X. Bulk and bubble-scale experimental studies of influence of nanoparticles on foam stability. *Chin. J. Chem. Eng.* **2017**, *25*, 347–357. [\[CrossRef\]](#)
185. Yekeen, N.; Manan, M.A.; Idris, A.K.; Mohamed, A.; Samin, A.R.R. Influence of silicon oxide and aluminum oxide nanoparticles on air and CO₂ foams stability in presence and absence of oil. *Chem. Eng.* **2017**, *56*, 1243–1248.
186. Cui, Z.-G.; Cui, Y.-Z.; Cui, C.-F.; Chen, Z.; Binks, B. Aqueous foams stabilized by in situ surface activation of CaCO₃ nanoparticles via adsorption of anionic surfactant. *Langmuir* **2010**, *26*, 12567–12574. [\[CrossRef\]](#)
187. Lee, D.; Cho, H.; Lee, J.; Huh, C.; Mohanty, K. Fly ash nanoparticles as a CO₂ foam stabilizer. *Powder Technol.* **2015**, *283*, 77–84. [\[CrossRef\]](#)
188. Singh, R.; Gupta, A.; Mohanty, K.K.; Huh, C.; Lee, D.; Cho, H. Fly Ash Nanoparticle-Stabilized CO₂-in-Water Foams for Gas Mobility Control Applications. In Proceedings of the SPE annual technical conference and exhibition, Houston, TX, USA, 28–30 September 2015.
189. Zhang, T.; Davidson, D.; Bryant, S.L.; Huh, C. Nanoparticle-stabilized emulsions for applications in enhanced oil recovery. In Proceedings of the SPE improved oil recovery symposium, Tulsa, OK, USA, 24–28 April 2010.
190. Zhang, T.; Roberts, M.; Bryant, S.L.; Huh, C. Foams and emulsions stabilized with nanoparticles for potential conformance control applications. In Proceedings of the SPE International Symposium on Oilfield Chemistry, The Woodlands, TX, USA, 20–22 April 2009.
191. Son, H.; Kim, H.; Lee, G.; Kim, J.; Sung, W. Enhanced oil recovery using nanoparticle-stabilized oil/water emulsions. *Korean J. Chem. Eng.* **2014**, *31*, 338–342. [\[CrossRef\]](#)
192. Zhang, T.; Espinosa, D.; Yoon, K.Y.; Rahmani, A.R.; Yu, H.; Caldelas, F.M.; Ryoo, S.; Roberts, M.; Prodanovic, M.; Johnston, K.P. Engineered nanoparticles as harsh-condition emulsion and foam stabilizers and as novel sensors. In Proceedings of the Offshore Technology Conference, Houston, TX, USA, 2–5 May 2011.
193. Khosravani, S.; Alaei, M.; Rashidi, A.; Ramazani, A.; Ershadi, M. O/W emulsions stabilized with γ -alumina nanostructures for chemical enhanced oil recovery. *Mater. Res. Bull.* **2013**, *48*, 2186–2190. [\[CrossRef\]](#)
194. Nguyen, N.; Tu, T.; Bae, W.; Dang, C.; Chung, T.; Nguyen, H. Gelation time optimization for an HPAM/chromium acetate system: The successful key of conformance control technology. *Energy Sour. Part A Recovery Util. Environ. Eff.* **2012**, *34*, 1305–1317. [\[CrossRef\]](#)
195. Cordova, M.; Cheng, M.; Trejo, J.; Johnson, S.J.; Willhite, G.P.; Liang, J.-T.; Berkland, C. Delayed HPAM gelation via transient sequestration of chromium in polyelectrolyte complex nanoparticles. *Macromolecules* **2008**, *41*, 4398–4404. [\[CrossRef\]](#)
196. Jang, H.Y.; Zhang, K.; Chon, B.H.; Choi, H.J. Enhanced oil recovery performance and viscosity characteristics of polysaccharide xanthan gum solution. *J. Ind. Eng. Chem.* **2015**, *21*, 741–745. [\[CrossRef\]](#)
197. Sveistrup, M.; van Mastrigt, F.; Norrman, J.; Picchioni, F.; Paso, K. Viability of biopolymers for enhanced oil recovery. *J. Dispers. Sci. Technol.* **2016**, *37*, 1160–1169. [\[CrossRef\]](#)
198. Bai, B.; Zhou, J.; Yin, M. A comprehensive review of polyacrylamide polymer gels for conformance control. *Pet. Explor. Dev.* **2015**, *42*, 525–532. [\[CrossRef\]](#)
199. Pérez-Robles, S.; Cortés, F.B.; Franco, C.A. Effect of the nanoparticles in the stability of hydrolyzed polyacrylamide/resorcinol/formaldehyde gel systems for water shut-off/conformance control applications. *J. Appl. Polym. Sci.* **2019**, *136*, 47568. [\[CrossRef\]](#)
200. Michael, F.M.; Fathima, A.; Alyemni, E.; Huang, J.; Almohsin, A.; Alsharaeh, E.H. Enhanced PAM Polymer Gels Using Zirconium Hydroxide Nanoparticles for Water Shutoff at High Temperatures: Thermal and Rheological Investigations. *Ind. Eng. Chem. Res.* **2018**, *57*, 16347–16357. [\[CrossRef\]](#)

